Title

Following the thread: Mytilus mussel byssus as an inspired multi-functional biomaterial

Journal

Canadian Journal of Chemistry, 100(3)

ISSN

0008-4042

Authors

Waite, J Herbert

Harrington, Matthew J

Publication Date

2022-03-01

DOI

10.1139/cjc-2021-0191

Peer reviewed

J_ID: CJC ART NO: cjc-2021-0191 Date: 10-January-22 Page: 1 Total Pages: 16 4/Color Figure(s): "F1-F7"

Pagination not final (cite DOI) / Pagination provisoire (citer le DOI)

Canadian Science Publishing

INVITED REVIEW

Following the thread: *Mytilus* mussel byssus as an inspired multi-functional biomaterial

J. Herbert Waite and Matthew J. Harrington

Abstract: Over the last 15 years, the byssus of marine mussels (*Mytilus* spp.) has emerged as an important model system for the bio-inspired development and synthesis of advanced polymers and adhesives. But how did these seemingly inconsequential fibers that are routinely discarded in mussel hors d'oeuvres become the focus of intense international research. In the present review, we take a historical perspective to understand this phenomenon. Our purpose is not to review the sizeable literature of mussel-inspired materials, as there are numerous excellent reviews that cover this topic in great depth. Instead, we explore how the byssus became a magnet for bio-inspired materials science, with a focus on the specific breakthroughs in the understanding of composition, structure, function, and formation of the byssus achieved through fundamental scientific investigation. Extracted principles have led to bio-inspired design of novel materials with both biomedical and technical applications, including surgical adhesives, self-healing polymers, tunable hydrogels, and even actuated composites. Continued study into the byssus of Mytilid mussels and other species will provide a rich source of inspiration for years to come.

Key words: bio-inspired materials, mussel byssus, DOPA-catechol, metal coordination, adhesion.

Résumé : Au cours des 15 dernières années, le byssus des moules marines (*Mytilus* spp.) est devenu un système modèle important pour le développement et la synthèse de polymères et d'adhésifs de pointe inspirés de la nature. Mais comment ces fibres en apparence sans intérêt, qui sont systématiquement jetées aux ordures lors de la consommation de moules en hors-d'œuvre, sont-elles devenues le centre d'intenses activités de recherches à l'échelle internationale? Dans la présente revue de littérature, nous adoptons une perspective historique pour comprendre ce phénomène. Notre objectif n'est pas de faire une synthèse du corpus substantiel de publications sur les matériaux inspirés des moules, car de nombreuses et excellentes revues couvrent déjà le sujet en profondeur. Nous explorons plutôt comment le byssus est devenu un objet de fascination pour la science des matériaux bio-inspirés, en portant une attention particulière à certaines percées qui ont permis de comprendre la composition, la structure, la fonction et la formation du byssus à partir de recherches scientifiques fondamentales. Les principes dégagés ont conduit à la conception bio-inspirée de nouveaux matériaux aux applications biomédicales et techniques diverses, dont des adhésifs chirurgicaux, des polymères autocicatrisants, des hydrogels réglables et même des composites activables. L'étude du byssus des moules de la famille des mytilidés et d'autres espèces est en voie de constituer une riche source d'inspiration pour les années à venir. [Traduit par la Rédaction]

Mots-clés : matériaux bio-inspirés, byssus de moule, DOPA-catéchol, coordination de métaux, adhesion.

The muddled history of mussel byssus

Mussels and mankind would seem to have nothing in common, but actually they do. Both live in tight, perpetually anxious communities, both are obsessively interconnected, and both are guilty of prolific consumerism. Perhaps these are just the ravings of researchers who have spent too much time investigating the byssus, a multipurpose holdfast made by mussels (Mollusca, Mytilidae). Indeed, byssus is the commodity that manifestly enables mussel community, networking, and consumerism. Of course, mussels acquired their behaviors long before the hominids. Humans consumed mussels since prehistoric times, but with the progression of civilization came appetites for more than mussel food. Some mussel species were prized for their byssal threads, which in the eastern Mediterranean region were spun into silken threads and woven into luxurious berets, purses, gloves, and stockings beginning perhaps in Hellenistic times (350 BC) and continuing to nearly the 20th century.[1] In recent years, scholarly interest in mussel byssus has mushroomed into a sprawling series of scientific and technological initiatives vying to capture or harness the secrets of mussel tenacity and wet adhesion. We aspire in this review to delineate scientific interest in the byssus and to describe where it stands today.

Recorded scholarly interest in mussel byssus started with Aristotle's *Historium Animalium* in which he pedantically noted that *Pinna* mussels were "affixed to the bottom (βυσσοῦ)" of the sea. In a popular translation by Theodorus Gaza (1400–1475), this description was corrupted and embellished to "affixed by a byssus (βύσσος)", a fine plant-derived linen of the ancient world.[2] The corrupted version percolated among scholarly circles for about 300 years. Réaumur[3] and de Heide[4] did not mention byssus in their detailed anatomical drawings of mussel holdfasts,

Received 12 July 2021. Accepted 27 September 2021.

J.H. Waite. Marine Sciences Institute, Lagoon Road, University of California, Santa Barbara, CA 93106, USA.
M.J. Harrington. Department of Chemistry, McGill University, 801 Sherbrooke Street West, Montreal, QC H3A 0B8, Canada.
Corresponding authors: J. Waite (email: hwaite@ucsb.edu) and Matthew Harrington (email: matt.harrington@mcgill.ca).

This paper is part of a special issue dedicated to the Department of Chemistry, McGill University, in honour of the bicentennial year of the founding of the university.

Fig. 1. Mussel in a beaker drawing by Antonio de Heide, 1684.[4] The foot (b) is just disengaging from a new plaque (eye-like ellipse, bottom center). Translation of title: "Anatomy of the Belgian Mussel that explains its elegant structure and amazing movement". [Colour online.]

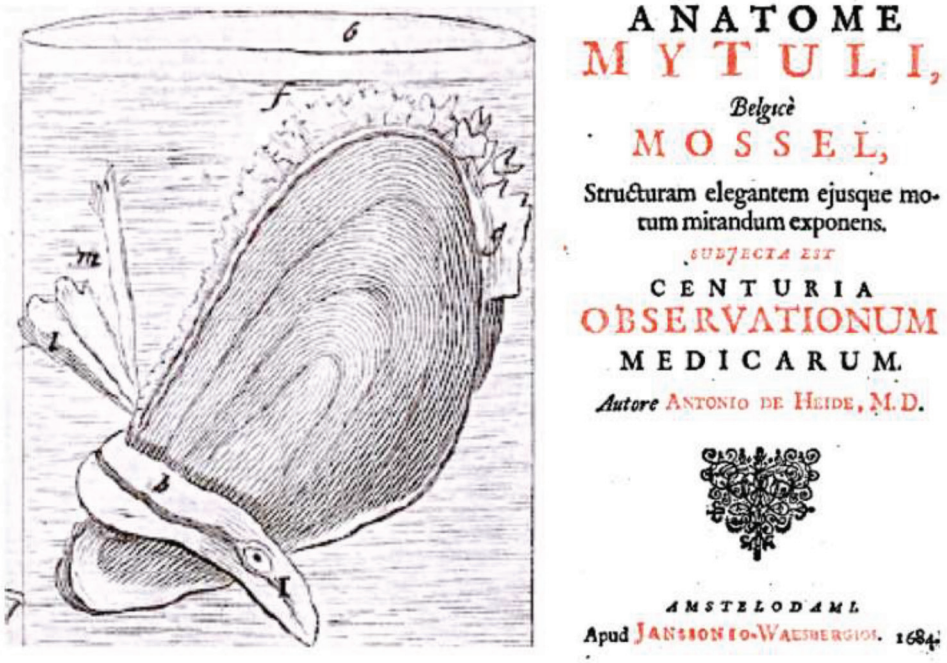

F1 although de Heide considered the holdfast a plant (Fig. 1). Mueller,[5] however, adopted byssus for the mussel holdfast and, after him, so did everyone else. Was Gaza's corruption suggesting a plant fiber intended to stoke more interest in mussel byssus than Aristotle's original meaning could? Perhaps he had an investment in the byssal silk trade? The questions remain moot.

In 1872, Anton Dohrn's endowment to establish the Zoological Laboratory, now the Stazione Zoologica di Napoli, energized marine biology by introducing sea creatures including mussels to visiting scientists, as well as providing the bench space to study them. Many researchers with interests in byssus anatomy, physiology, biochemistry, and biomechanics such as Tullberg,[6] Seydel,[7] Stary and Andraschke,[8] and others too numerous to mention availed themselves of this heaven-sent facility. Within a score of years, similar laboratories were built in the US, Britain, and France and were crucial in enabling the transfer of the latest histochemical and fiber X-ray advances in the medical sciences to marine biology generally and mussels particularly.[9,10] With regard to adventitious histochemistry, there was an amusingly erroneous though prescient report by Tullberg in 1877 in which he marveled at finding a green gland in a mussel foot following fixation in cognac and sectioning.[6] Although the green color was an artifact of the acidity and iron impurities in the cognac (during distillation), his result anticipated the popular green ferric chloride stains used later for detecting polyphenols in both foot and byssus material.[11]

Biomimetics

The biomimetic phase of mussel byssus started much earlier — in the 1940s — than most are aware. It was not an institutional program but rather a coalescence of the multidisciplinary interests of Mark G.M. Pryor, Laurence E.R. Picken, Norman de Bruyne, and others spurred by the war effort. Pryor was a senior tutor and Fellow of Trinity College and in the Department of Zoology, Cambridge University and had considerable though divergent expertise in zoology and aircraft construction, the latter wittily described in *The New Science of Strong Materials*,[12] so it was natural for him to look for common themes in the two. Pryor's focus on multi-ply fiber-filled insect cuticles undoubtedly led to inclusion of these in discussions about composite lightweight aeronautical material designs. Picken, a Fellow of Jesus College and a graduate research advisor in Zoology at Cambridge, was a pioneer of investigating the multiple length scales of structure in biopolymers.[13] Norman de Bruyne of the Royal Aircraft Establishment (RAE) Farnborough was a founding father of modern adhesion science. He started with Ernest Rutherford at the Cavendish Laboratory in Cambridge before spinning off several aircraft companies and personally building two high-performance airplanes using layers of balsa wood or linen impregnated with glue. In 1940, Pryor's discovery of a pathway for quinone-tanning (QT) in insects that led to sclerotization of the exoskeleton put him on the map.[14] It identified the cross-linker needed harden the protein–chitin mixtures (Fig. 2A). Alexander Todd and others helped Pryor characterize the tanning agent as protocatechuic acid and showed that oxidation to *o*-quinone made it a very versatile cross-linking agent.[15,16] De Bruyne's switch from casein to phenol- or resorcinol-formaldehyde glues in aircraft construction coincided with these discoveries and was informed by them. Multi-talented and decorated research clusters were not uncommon in Cambridge at the time. Baron Lord Todd, Nobel Laureate (for synthesizing ATP and flavin), was Master of Christ College, Cambridge. Pryor was himself a grandson of a baronet and married to Sophie Raverat, a talented artist and a great granddaughter of Charles Darwin, and, finally, Picken was a world traveler, ethnomusicologist of traditional Chinese and Turkish music, and a polymer physicist. The Cambridge teams' rigor and panache in describing catechols as the keystone of insect sclerotization made QT an instant shibboleth for the greater zoology and biomaterials research community, though not always with adequate justification. Indeed, Julian Vincent, to his credit, has often questioned the universality of the QT pathway proposed by Pryor thereby stoking curiosities about other catechol-mediated pathways.[17] F2

Fig. 2. Comparing (A) Pryor's and (B) Brown's deductions about the disposition and role of catechols in insects and mussels. Both biomaterials, eggcase and byssus, were observed to consist of catechols, resin proteins, and fiber filler. The major difference between the two is that insect catechols were low molecular weight and needed to be enzymatically deblocked, whereas in mussels, catechols were already fused to the resin proteins. Much more is now known about both pathways. [Colour online.]

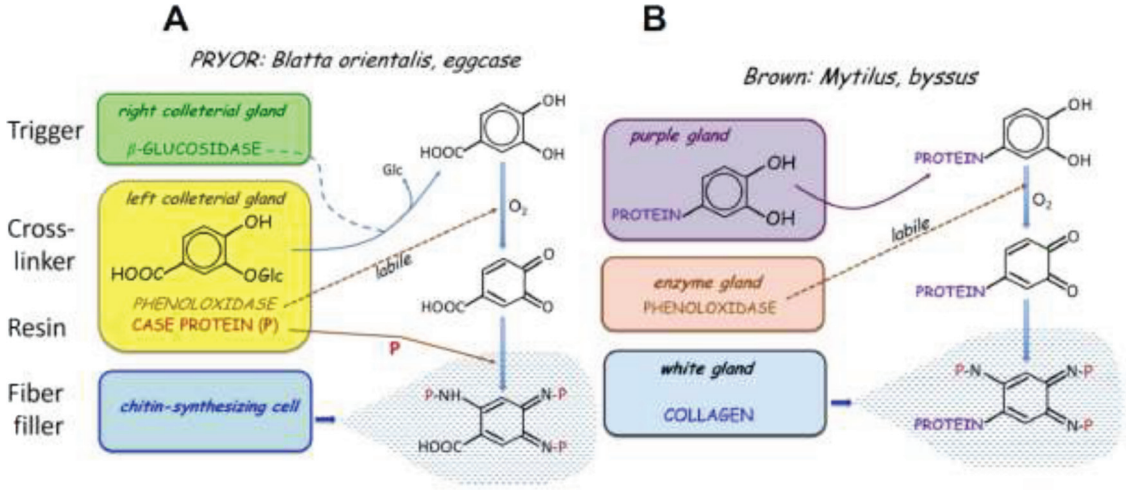

C.H. Brown: Byssus in the crosshairs

While at RAE Farnborough during the Second World War, Pryor met a student intern C.H. Brown from Girton College, Cambridge, on a National Service assignment to help improve the design of RAF pilot helmets (correspondence, Girton College Archives). When Brown expressed interest in his work on natural load-bearing composites of fiber-reinforced phenolic resins, he apparently suggested *Mytilus* byssus to her as a promising project for studying QT in marine organisms. Brown was smart, scholarly, and independent, but also intensely reserved, rarely revealing more about herself than her initials C.H. Between ~1944 and 1949, with Pryor and Picken as mentors and *Mytilus* as her model organism, she succeeded in showing or adding substance to the following: (*i*) byssal threads contain collagen but extend much more than tendon, (*ii*) byssal threads and foot both contain high-molecular weight catecholic compounds, and (*iii*) byssal catechols are covalently tethered to proteins and readily bind to Fe^{III}.[11] These were important deviations from Pryor's model of QT in insects and gave mussel byssus its own stamp (Fig. 2B). Brown gained her PhD from Cambridge in 1950 and between then and 1955 published four noteworthy single-author papers.[11,18–20] In 1950, she also married William Ranulf Brock, a lecturer of US History at Cambridge; then in 1955, distracted by domestic demands and two children, she exited from the world of laboratory research.

Pryor, though continuing as Senior Tutor at Trinity, also stopped publishing after 1955 for unknown reasons. In 1967, he suffered a head injury in a car accident that left him in a vegetative coma until he passed away in 1970 at age 51. In the foreword to her extraordinary Lazarus-like treatise "*Structural Materials in Animals*",[21] Brown wrote of Pryor: "It was he who directed my interest towards this subject and whose suggestions helped shape many of my ideas". Alas, the mussel muse never returned to mussels or catechols and finally passed away in 2000.

Emergence of byssus biochemistry

As a graduate student in Zoology at Duke University in the 1970s, Waite was mesmerized by Brown's 1952 paper on structural proteins in *Mytilus*. Everything was so concisely and accurately articulated, so well poised for continuation. If there was any criticism, it was that Brown was parsimonious with illustrations of her analytical data; perhaps photographs were prohibitively costly to make and print at the time. Brown's only research support came through a string of student fellowships. Waite knew of few other biological processes or organisms that involved such a generous stockpile of precursors or speedy assembly than byssal thread formation by mussels (Fig. 3). As there were no reports of efforts after Brown's 1952 paper, Waite accepted her and Pryor's wordless invitation to carry on. In 1976, he got an NSF–NATO Fellowship to study mussel byssus with S.O. Andersen in Copenhagen and thus began a long series of peculiar protein characterizations that did not slow down until 2017. F3

Given a mussel's ability to make a new thread every 1–5 min, a stockpile of byssal precursors had to exist in the mussel foot glands (Fig. 3). Brown[11] and later Smyth[22] predicted three types of stored proteins: collagen from the collagen gland, catecholoxidase from the accessory or enzyme gland, and catecholic proteins from the accessory and phenol gland. Catecholoxidase activity was detected in the foot but the enzyme proved unstable and still awaits proper characterization.[23] Brown[11] mentioned a sensitive and specific stain for tissues bearing catechols based on exposure to nitrous acid followed by alkaline pH. Unbeknownst to her, this reaction had been adapted by Arnow[24] for analytical solution chemistry and could easily distinguish 3,4-dihydroxyphenyl-L-alanine (Dopa) from Tyr and Trp. Using 5% acetic acid for extraction, Waite identified two catecholic mussel foot proteins (mfp), mfp-1 and mfp-2, simply by applying the Arnow reaction to acid-extracted proteins separated by electrophoresis in polyacrylamide gels. Mfp-1 is from the accessory (or enzyme) gland, consists of short, tandemly repeated sequences, and contains high levels of Dopa and modified prolines.[25–27] Mfp-2 is from the phenol gland and has a sequence with longer tandem repeats and Dopa lightly distributed throughout.[28,29] Neither mfp-1 nor mfp-2 proved to be particularly good adhesives, though mfp-1 found a market niche as a cell and tissue culture attachment factor that persists to this day (BD Cell-Tak™). 5% acetic acid extractions of *M. edulis* mussel feet also liberated collagens or preCols, which will be described below in more detail.[30] These too contained Dopa, but only at their N- and C-termini. AQ1

For reasons still not understood today, the really sticky adhesive mfp proteins require more aggressive extraction conditions for liberation from mussel foot tissue. For example, the mfp-3 variant family requires 5% acetic with 8M urea for release,[32] and mfp-5 is liberated by 5% acetic acid with 6M guanidine·HCl.[33] These are highly DOPA-rich precursors at 20 and 30 mol %, respectively. Mfp-3 variants encompass a large family of up to 30 isoforms

Fig. 3. Relationship between the mussel foot and production of a new byssal thread. Each thread consists of a core shaft, cuticle, and plaque. New threads are injection-molded on demand in the pedal groove and distal depression of the foot from precursors stockpiled in three glands, which were variously known as the phenol (purple), collagen (white), and accessory (enzyme) glands. Two-foot slices — one proximal and one distal — stained by Arnow's method, show catechols distributed throughout the foot core but reaching the highest levels in the accessory and phenol glands. The distribution of eight foot-derived proteins, all Dopa-containing, is shown. Mfp, mussel foot protein; TMP, thread matrix protein; preCol pre-pepsinized collagen. Adapted with permission from Demartini et al. 2017.[31] [Colour online.]

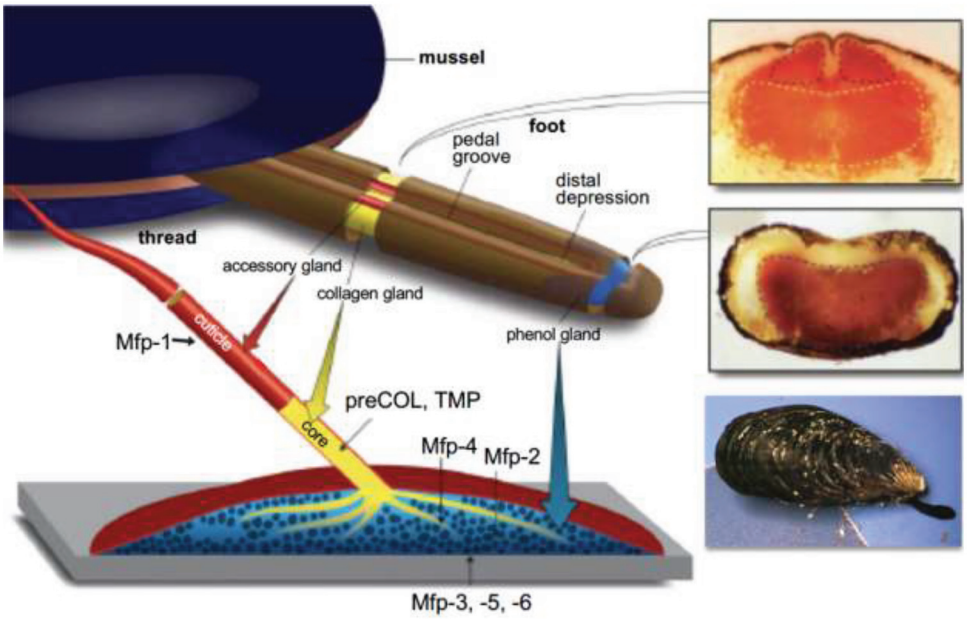

and, besides DOPA, contain significant amounts of another unusual modification, 4-hydroxyarginine. Besides Dopa, Mfp-5 contains variable amounts of *O*-phospho-serine. Both proteins are made and stored in the phenol gland,[27,34] and upon secretion, both are confined to byssal plaques near the substrate interface.[35,36] Known Mfp localization in foot and plaque is schematically summarized in Fig. 3.

Discovery of mfp-5 with high levels of Dopa, Lys, and Gly was a watershed moment, because it put the protein on the same plain as many engineered random block copolymers with compositions dominated by a few functionalities, e.g., Dopa, Lys, and Gly. Then came two additional insights: (*i*) Dopa-bound metal ions such as Fe^{III} serve as cross-linking surrogates,[37–39] and (*ii*) a single cantilever-tethered Dopa exhibited covalent-like but reversible binding to titania surfaces based on atomic force microscopy.[40] In the ensuing pandemonium, research on mussel byssus splintered into groups focusing on collagens, metal ion binding, and individual mfps in adhesion. The golden age of byssus research had begun.

Progress in the last 30 years — the golden age of byssus research

Stimulated by advances in the biochemical understanding of the byssus, a surge in efforts to establish structure–function relationships between the chemical peculiarities of the byssus and their impressive material function followed. These studies have evolved hand in hand with the field of mussel-inspired synthetic materials,[41–43] and the feedback between biological and biomimetic efforts has been highly conducive to progress on both sides. Below, we will tell the story of how the secrets of the byssus were unlocked with sections focusing on the three most prominent functional parts of the byssus — namely, the core, cuticle, and plaque. We conclude with an overview of past and present efforts to understand the fabrication process by which byssal threads are made.

The byssal thread core — a tough and self-healing tether

Functional characterization

Functionally, the byssal thread fiber acts as a tether between the adhesive plaque and the stem, which anchors directly into the soft tissue of the mussel (Fig. 4). As such, the tensile properties of these fibers are extremely relevant for their role in anchoring mussels to hard surfaces where incessant and cyclic application of intense hydrodynamic forces presents a dominant selective pressure. Denny and Carrington investigated the "ecomechanics" of the high intertidal zone utilizing a clever device for mimicking and measuring what organisms experience in the intertidal, showing that water velocities can reach 10 m/s with acceleration approaching 400 m/s^2 — a formidable mechanical challenge for even the best man-made polymers.[45,46] Yet, mussel beds often remain firmly intact except during the biggest winter storms.[46]

Initial analysis of *Mytilid* byssal threads mechanics by Brown and Mercer focused mainly on the extensibility of the fibers,[11,47] while later studies by Vincent, Price, and others also reported values for material stiffness and strength using pull-to-break tensile studies.[48–50] While these investigations mainly focused on measuring whole thread mechanics, even at this stage it was recognized that the proximal (closest to the mussel) region of the thread was considerably more extensible than the distal region (closest to the surface). Later work by Gosline and Carrington more thoroughly examined the mechanical properties of the proximal vs. distal region, demonstrating that the distal portion of threads of *M. californianus* is more than 50-fold stiffer, about 2-fold stronger, and about half as extensible compared with the proximal region (Fig. 4E).[51–53] Importantly, the shape of the stress–strain curves deviates significantly between the distal and the proximal regions. The distal thread is initially stiff, with a clear yield point occurring at ~12% strain, followed by a post-

Fig. 4. Mussel byssus core. (A) Mytilus *californianus* mussel attached to a surface with its byssus. (B) SEM of byssal thread torn open showing core and cuticle. (C) Schematic of hierarchical organization of preCol proteins within the core. (D) Schematic of His–Zn metal coordination bond present in His-rich domains of preCols. (E) Pull-to-break stress–strain curves for the distal and proximal regions of byssal threads. (F) Cyclic stress–strain curve of distal thread, highlighting large hysteresis in the first cycle, damage in the second cycle, and self-healing response in the third cycle. Schematics indicate proposed double network model consisting of sacrificial bonds (His–Zn cross-links) and elastic network (cross-beta sheet flanking domains). Figure adapted from Reinecke et al. 2017 with permission.[44] [Colour online.]

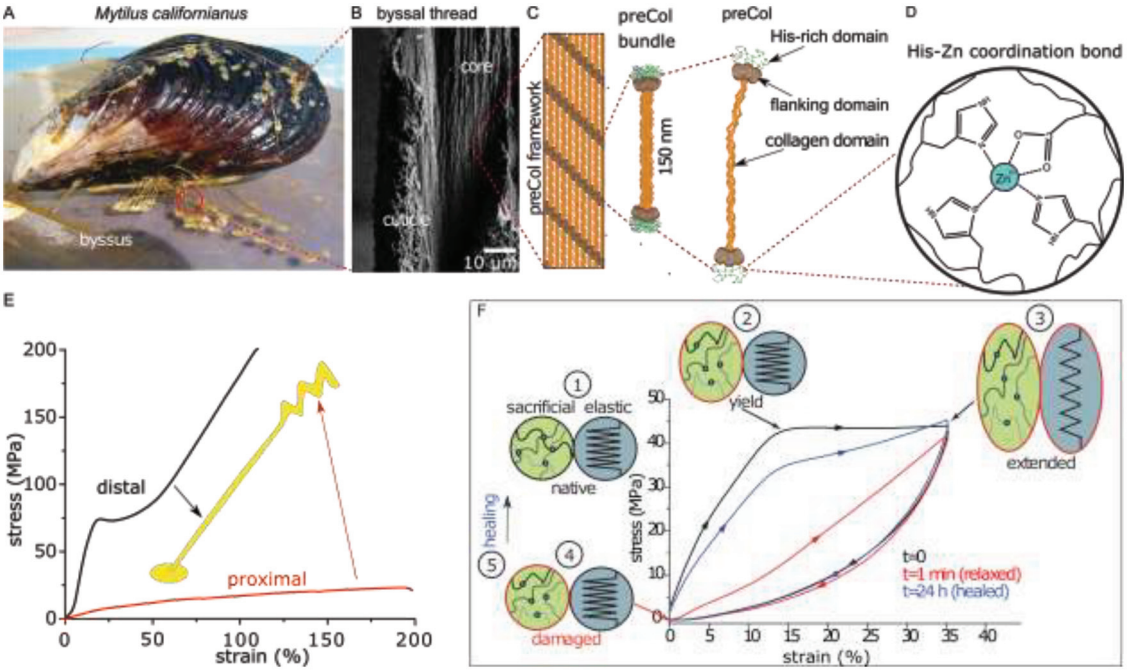

yield plateau until ~40% strain, after which the stress increases until failure at ~100% strain (Fig. 4E). The proximal thread, on the other hand, does not exhibit a yield point and continues to extend until ~200% strain.[51,52] Waite et al. proposed that the divergent mechanical response of the proximal and distal thread reflects a functional gradient that helps to mitigate stress concentrations due to modulus mismatch, considering that the byssus is essentially a direct link between stone (E ~10 GPa) and the soft tissue of the mussel (~200 kPa).[54] Thus, by gradually transitioning from stiff to soft, the byssus avoids localized failure at any abrupt transitions including the interface.

In the high intertidal zone, large waves can arrive with a period of just a few seconds,[55] and byssal threads seldom undergo failure upon first impact. Thus, cyclic mechanical testing of byssal threads to strains lower than the breaking strain revealed several other key characteristics relevant for their biological function (Fig. 4F). When cycled below their yield point, distal threads are highly resilient, resembling tendon, with only 9% hysteresis observed.[51,54,56] In contrast, when cycled beyond their yield point, distal threads exhibit a mechanical hysteresis of up to 72% (e.g., when cycled to strains of over 60%),[51,54,56] enabling significant dissipation of energy from crashing waves. Although yield of synthetic polymeric materials is associated with permanent damage and residual strain, the distal threads, given sufficient time, can recover their initial length when load is removed. Subsequent loading cycles, however, exhibit significantly reduced stiffness and hysteresis (Fig. 4F).[51,54,56] The softening of the threads that are bearing the brunt of the load was proposed by Carrington and colleagues to functionally recruit other threads in the byssus, by effectively redistributing the load over a greater number of threads.[51] Remarkably, it was observed separately by the groups of Waite and Gosline that threads will recover back toward initial mechanical properties in a time-dependent self-healing process (Fig. 4F),[52,56,57] which later became a main focus on efforts for bio-inspiration.[58] It was determined that threads can recover up to 60% of initial stiffness and hysteresis after only 1 h and up to 80% recovery is possible in 1 d.[59] These time scales are relevant to the time spent during low tide, when mussels in the most wave-exposed regions are given a break of several hours, and it was observed that healing rate increased with temperature.[59] Cyclic loading of the proximal region also exhibits a notable hysteresis (47%), but in contrast to the distal region, it increases in stiffness with increasing number of loading cycles.[52,60]

Compositional characterization

Prior to the advent of specific compositional analyses, early byssus enthusiasts had speculated upon the constitution of the byssal threads with de Heide even considering the byssus to be of plant origin as already mentioned[4] and Gaza calling it “lana illa pinnali” or Pinna wool.[2] However, initial histological analysis of *Mytilus* threads already hinted at their collagenous composition,[11,61,62] which was further supported by studies of the precursor proteins within the mussel foot. For example, it was found that collagenase enzymes were capable of digesting the contents of the collagen secretory vesicles used to form the thread.[63] However, initial efforts to extract proteins directly from the thread were unsuccessful, presumably due to the cross-linking of the proteins.[11] This challenge was eventually overcome by the group of Waite who acquired the sequence of the byssus fiber proteins by first digesting threads with pepsin, resulting in the purification of three different partial collagen-like sequences that were pepsin resistant.[30,64–66] The full-length sequences of the three proteins were acquired from cDNA libraries, which were given the name pre-pepsinized collagens, shortened to preCols.[30]

Each of the three preCol variants consists of multiple domains including a large central collagen domain, flanking domains on either side resembling various structural motifs and domains enriched in histidine at both the N and C termini (Fig. 4C).[61] The collagen domains were unusual in containing several breaks in the canonical collagen Gly-X-Y triplet motif, which were proposed to result in kinking of the rod-like collagen domains.[67] The flanking domains of the three variants, which are known as preCol-D, preCol-NG, and preCol-P, have sequence motifs that resemble dragline silk-like polyalanine runs, Gly-rich flagelliform silk sequence, and elastin, respectively.[30] Finally, the histidine-rich domains contain ~20 mol% His, which given the elevated content of transition metal ions in the threads (Zn and Cu) were proposed to participate in forming metal coordination complexes (Fig. 4D).[30,56,57] Interestingly, it was revealed that the different variants are not uniformly distributed in the different parts of the fiber with preCol-D concentrated in the distal region, preCol-P concentrated in the proximal region, and preCol-NG essentially constant along the length, leading to the proposal that this compositional gradient may determine the difference in mechanical properties in proximal vs. distal thread.[53] Further compositional analysis of the thread by the Waite group revealed that the core also contains at least two different non-collagenous matrix proteins known as thread matrix protein-1 (TMP-1) and proximal thread matrix protein-1 (PTMP-1), which are unevenly distributed along the length of the thread, also possibly contributing to the mechanical gradient.[68,69]

Structural characterization

In line with the compositional analysis, early X-ray diffraction work by Mercer, Rudall, and others not only provided evidence of a primarily triple helical collagenous structure in the thread,[46,70] but also suggested the presence of beta proteins. However, TEM imaging of threads by numerous groups did not show the typical 64–67 nm banding pattern of type I fibrillar collagen, suggesting the higher length-scale organization of the byssal collagen was very different from other collagenous fibers.[71] Indeed, TEM of the distal region showed highly aligned fibrils with a lateral spacing of 8–9 nm, while the fibrils in the proximal region exhibited an undulating morphology, with a non-fibrillar material between the fibrils.[71] These differences in alignment were clearly observable in polarized light microscopy as well.[72] TEM imaging further suggested that the collagen molecules were organized in 6+1 hexagonal bundles, which was further supported by AFM imaging (Fig. 4C).[67] Small angle X-ray scattering (SAXS) measurements of the distal thread by the group of Harrington confirmed that the preCols were arranged in 6+1 hexagonal bundles and that the bundles within the threads were further arranged in a quasi-hexagonal organization.[73] Axially, the preCol bundles were deduced from SAXS experiments to be arranged end-to-end with adjacent fibrils staggered relative to one another with a periodicity of 13 nm (Fig. 4C).[73] Synchrotron wide-angle X-ray diffraction (WAXD) studies confirmed a triple helical conformation resembling that of tendon, with the additional presence of a conspicuous meridional reflection indicating cross beta sheet structure.[54,59] The identified beta sheet conformation, which confirmed earlier speculations from the 1950s, was further supported using both FTIR[74] and solid state NMR[75] spectroscopy and was proposed to arise from the silk-like flanking domains of preCol-D.

Structure–function relationships

The ultimate goal of these studies stretching back over 70 years was to establish clear connections between the composition, structure, and mechanical function of these fibers — yet, a detailed understanding remained elusive even until more recently. The peculiar byssal collagens with their flanking domains and His-rich domains[30] led to many provocative hypotheses as to why the mechanics of the byssus diverge so significantly from that of tendon. Eventually, application of synchrotron X-ray radiation provided a means of testing these hypotheses directly by enabling the combination of in situ mechanical and structural analysis, tying specific features of the byssus stress–strain curves to specific changes in the conformation and cross-linking of the byssus core proteins. Collaboration between the Waite and Fratzl research groups combined synchrotron WAXD measurements with in situ cyclic loading of threads, revealing that the collagen domain is only extended by 2% molecular strain even while the thread is extended to strains of 70%.[59] This indicated that the large extensibility of the byssal threads must arise from unfolding of protein structure in the flanking domains and HRDs based on the knowledge that preCols are organized into fibrils packed tightly in the fiber core. Harrington's group later confirmed this hypothesis by focusing on changes in specific WAXD diffraction peaks for the cross-beta sheet structure, which was deduced to unfold during stretching and refold rapidly upon unloading.[44,74] SAXS measurements combined with cyclic loading provided a higher order view of this unfolding process showing that the unraveling of the flanking domains occurs in a stepwise process.[73] In subsequent cycles showing decreased stiffness, this transition was not observed — the transition occurs smoothly, which was attributed to the presence of sacrificial bonds that are broken in the first cycle and not fully recovered in the second cycle, but which recover over time in a self-healing event (Fig. 4F).

The primary candidate for sacrificial bonding in the thread were the metal coordination bonds between histidine residues in the HRDs and transition metal ions known to be present in the byssus, including Zn and Cu.[57,76] Support for this hypothesis came initially by studies in which threads were mechanically tested after undergoing various treatments targeting the integrity of the His-metal complexes, including metal chelation with EDTA, histidine protonation with pH, and histidine modification with diethylpyrocarbonate (DEPC).[56,57] Perhaps most convincingly for the role of histidine in mechanics, threads exhibited a sigmoidal decrease in stiffness from 800 MPa to 400 MPa that almost perfectly matched the titration curve of histidine — notably, histidine does not bind metal ions efficiently when protonated at acidic pH.[56] Furthermore, threads that were stretched and then rested in acidic buffers lost their ability to self-heal in comparison with control fibers in seawater.[59] Strong evidence for the presence and mechanical role of His-Zn coordination bonds was finally acquired by the group of Harrington using X-ray absorption spectroscopy (XAS) with EXAFS analysis combined with mechanical testing.[77] These studies revealed that on average Zn ions in the threads had a coordination number of 5, with three His residues and one Asp residue as direct ligands (Fig. 4D). When stretched to the end of the yield plateau, it was deduced that several amino acid ligands were replaced by water molecules, consistent with bond rupture. When load was removed, the metal coordination sites were again filled with amino acid ligands; however, the bond lengths were considerably strained compared with the native state. Over time, the bond structure recovered toward the native configuration suggesting that healing involves the formation of an optimal network topology.[77] Combined with the hidden length of the cross-beta sheet structure, these reversibly sacrificial bonds provide a means of dissipating significant mechanical work via rupture of metal coordination cross-links, while the refolding of the beta sheet plus the reorganization of the metal bond network provide the means for self-healing (Fig. 4F).[44,77] These concepts provide fertile ground for developing bio-inspired self-healing polymers.

These findings explained to a large degree the behavior of the distal region of the thread but not the large difference in the mechanics of the less studied proximal region. Along these lines, it was proposed that the mechanical variation between the distal and proximal regions was largely controlled by the gradient of

preCol-P and preCol-D.[30,54] Specifically, it was hypothesized that the elastin-like sequence of the preCol-P flanking domain results in a more extensible mechanical behavior in comparison with the silk-like domains of preCol-D. Fibers produced in vitro from purified preCol with different proportions of preCol-P and preCol-D showed that at least part of the mechanical difference could be explained by this;[78,79] however, the clear ultrastructural differences between the proximal and distal region and the larger content of PTMP-1 in the proximal region will also play a large role.[69,71]

Investigation of the thread cuticle — a hard and extensible abrasion-resistant coating

Functional characterization

Byssal threads from *Mytilus* and related genera possess a thin outer coating known as the cuticle that is compositionally, structurally, and mechanically distinct from the inner core of the threads (Figs. 4B, 5A–5C).[37,81] The cuticle, initially referred to as the tanned border or cortical layer, was first noted by Bairati and Vitellaro-Zuccarello[71] about 45 years ago, but at that point, no special attention was given to this thin veneer. The first functional studies of the cuticle were initiated by Holten-Andersen and Waite in which they explored the hypothesis that the byssus cuticle might play a role in abrasion resistance against sandblasting in the marine intertidal.[81–83] It was determined through nanoindentation that the cuticle of *M. galloprovincialis* and *M. californianus* possessed hardness and stiffness values comparable with common engineering epoxies, while microcracking studies revealed species-dependent extensibilities of up to 100% strain before cracks propagated through the cuticle.[81] It was hypothesized that the hard coating functions to protect the softer core of the thread and that the high extensibility is adapted to match the high ultimate strain of the fiber core. This combination of hardness and stretchability is unmatched in typical engineering materials and thus presented an exciting role model for bio-inspiration.

Compositional characterization

The most prominent protein component of the cuticle is mussel foot protein-1 (mfp-1), and for quite some time, it was the only cuticle protein identified (Fig. 4H). Originally, purified and characterized by Waite and Tanzer in 1981, mfp-1 was initially believed to be an adhesive protein[84] but was later localized specifically to the cuticle.[85] As mentioned above, the mfp-1 sequence consists of ~80 tandem repeats of AKP*SY*P**P*TY*K, where P*, Y*, and P**, respectively, are 4-trans-hydroxy-L-proline (Hyp), Dopa, and 2,3-trans-3,4-cis dihydroxy-L-proline (DHP).[25–27] Mfp-1 was considered to be peculiar at the time and the biochemical evidence for protein bound DOPA-catechol moieties caught the attention of many researchers, who would later pave the way for much of the field of mussel-inspired materials. It is appropriate to emphasize that mussels have no monopoly on protein DOPA; it is widely distributed in the structural materials of animals including molluscan periostracum and shell matrix, trematode eggshells, polychaete cement, tunicate test proteins, and selachian capsules.[86–89] Recent transcriptomic analysis of the accessory gland suggests that a number of cysteine-rich proteins may also be present in the cuticle,[31] with one — mfp-17 — confirmed to be in the cuticle secretory vesicles.[90]

In addition to cuticle proteins, Holten-Andersen provided spectroscopic evidence for the specific localization of metal ions, including Fe, concentrated in the cuticle.[82] Given the well-characterized tendency of catechols like DOPA to form highly stable catecholate coordination complexes with transition metals, it was posited that mfp-1 in the cuticle may be cross-linked via DOPA–metal bonds.[39,82] Direct evidence for this hypothesis was obtained using confocal Raman spectroscopic imaging of the native cuticle, revealing characteristic resonance Raman bands of the catechol–metal complex (Fig. 5G).[37] Notably these bonds were reversible since the metals could be largely removed with a metal chelator such as EDTA and recaptured by soaking EDTA-treated threads with metal ion solutions.[37,91] While initial studies ascribed these Raman spectra to DOPA–Fe coordination bonds, it was recently revealed that mussels also integrate and coordinate vanadium ions with mfp-1 perhaps preferentially over iron ions,[80] although mussels do appear to be opportunistic in terms of what metals they integrate into their byssus.[91]

F5

Structural characterization

The tanned border originally identified by Bairati and Vitellaro-Zuccarello referred to the outer coating of the whole thread including stem,[71] but the specific structure was not examined in detail at this point. A detailed TEM image of the structure of the "cortical layer" was presented by Vitellaro-Zuccarello showing for the first time that the bumpy surface of the cuticle of *Mytilus galloprovincialis* was due to the presence of small round inclusions with a mottled texture within a continuous homogenous phase (Fig. 5C).[92] Yet, following this basic ultrastructural analysis, very little was done to further investigate the byssus cuticle until over 25 years later when Holten-Andersen and Waite examined the cuticles of several different species, discovering that cuticle micro and nanostructure varied significantly between different species.[81–83] *Mytilus* species all possess the small spherical inclusions, termed granules, which are embedded in a continuous phase termed the matrix. Comparative interspecies analysis revealed that both the size and submicron texture of the granules varies between different *Mytilus* species and that certain *Perna* and *Modiolus* mussel byssal threads were found to be missing the granular substructure entirely.[81,83,93] For example, *M. edulis* and *M. galloprovincialis* possess granules of approximately 1 μm in diameter that possess a biphasic brain-like nanoarchitecture, while the granules in *M. californianus* have an average diameter of about 200 nm with no substructure visible in TEM.[80,81,83] Harrington's group studied the three-dimensional micro- and nano-scale structure of the *M. edulis* cuticle using focused ion beam scanning electron microscopy (FIB-SEM), revealing a bicontinuous network of 20 nm thick layers superficially resembling a block copolymer gyroid phase (Figs. 5I and 5J).[80] These studies were coupled with elemental analysis showing a strong vanadium signal coming from the granules, while the matrix was enriched in sulfur and iron (Figs. 5D and 5F). This was completely in line with resonance Raman studies that showed the localization of DOPA-V cross-links specifically at higher density in the granules than in the matrix,[37,91] while the localization of sulfur in the matrix suggests that this might be where the Cys-rich cuticle proteins such as mfp-17 are localized.[31,90]

Structure–function relationships

Even though the structure and composition of the cuticle are now much better understood, the structure–function relationships defining this material are incomplete. Holten-Andersen and Waite's pioneering studies of this material suggested that the high hardness of the cuticle arises from the granules, which act as hard inclusions, and that the high extensibility comes from the matrix, which exhibits reversible microcracking during tensile deformation that circumvents propagation of larger cracks through to the core.[81] Raman spectral mapping showing the elevated DOPA–metal cross-link density in the granules vis-à-vis the matrix supported this model of cuticle mechanics (Fig. 5G).[37] Monnier and Waite later proposed a modified model based on AFM-based nanoindentation of granules under semi-hydrated conditions suggesting that the granules retain a higher degree of water and actually behave softer than the matrix under these specific conditions.[93] In either case, studies by Harrington demonstrated that removal of metal ions from the cuticle with

J_ID: CJC ART NO: cjc-2021-0191 Date: 10-January-22 Page: 8 Total Pages: 16 4/Color Figure(s): "F1-F7"

Fig. 5. Mussel byssus cuticle. (A) Light microscopy image of stained byssus showing the cuticle (red) and core (blue). (B) SEM image of granular byssus cuticle (red) from *M. edulis* covering the fibrous core (blue). (C) TEM image of cuticle (red) showing the granules with their brain-like texture and matrix. (D)–(F) TEM-EDS images showing distribution of (D) sulfur, (E) iron, and (F) vanadium in the granules vs. matrix. (G) Confocal Raman image showing concentration of DOPA–metal cross-links in the granule vs. matrix with schematic of tris-DOPA-V complex. (H) Schematic of mfp-1 protein highlighting consensus decapeptide motif of the repetitive domain. (I) Three-dimensional reconstruction of several granules from FIB-SEM image stack showing internal brain-like texture. (J) Zoom in of one granule from (G) showing bicontinuous network structure inside granules. Figure adapted from Jehle et al. 2020 under the creative commons license (CC BY 4.0).[80] [Colour online.]

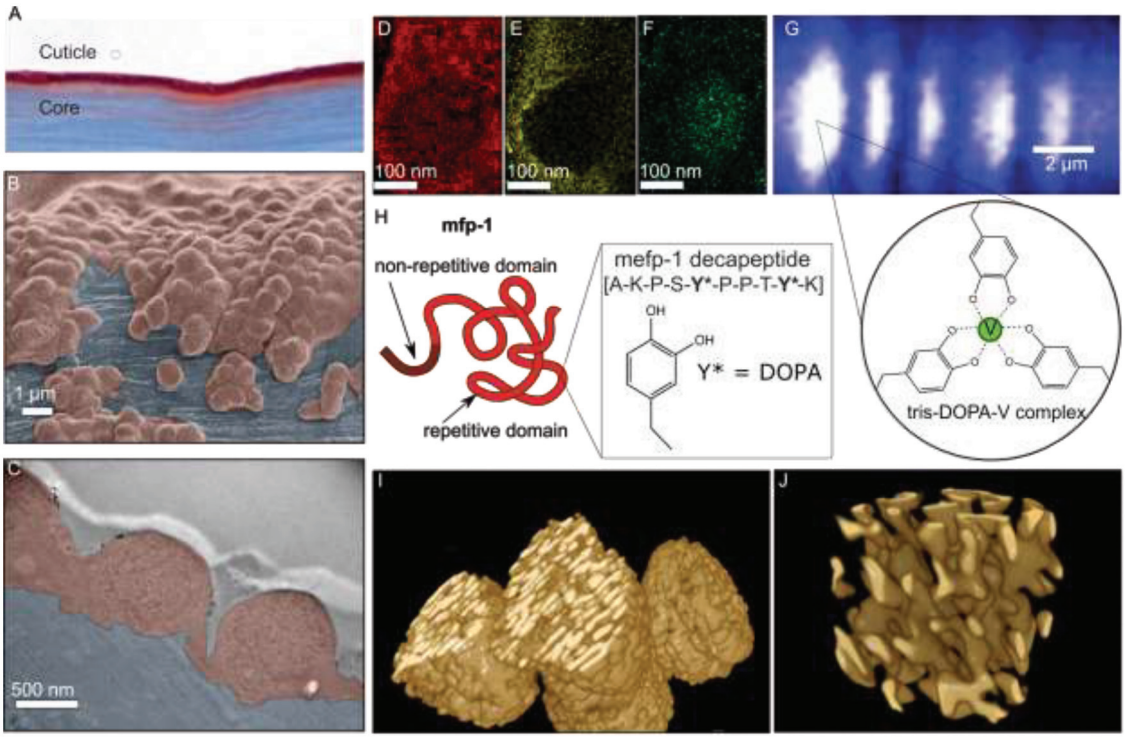

EDTA resulted in a decrease in both hardness and stiffness of the cuticle of over 80% based on nanoindentation analysis, which could be fully recovered by soaking the metal-depleted cuticle in metal chloride solutions of Fe, V, and Al.[91] Notably, EDTA treatment resulted in a loss of the resonance Raman spectral peaks for DOPA–metal coordination, which were recovered after metal replenishment.[65] This strongly suggests that the DOPA–metal coordination bonds, which are presumably localized in the granules, provide much of the cross-linking and that covalent bonds only make up a maximum of ~15% of total cross-links. Cohesion measurements between thin layers of mfp-1 in the presence of metal ions support this model of metal-dependent mechanics.[94,95] Indeed, very recent studies further indicate that DOPA-V complexation can provide a nearly two-fold increase of cohesive forces between layers of mfp-1, providing some insight into why this metal might be preferentially used to cross-link the hard granules.[95] Nonetheless, one must also consider the possibility that cysteine–metal interactions might be present in the matrix based on the co-localization of sulfur and Fe in elemental analysis studies[80] and that metal removal and recovery studies also affect the matrix mechanics. However, this remains speculation for the time being.

Investigation of the byssal plaque — a versatile glue for aquatic environments

Functional characterization

The ability of the byssus to securely adhere to wet marine intertidal surfaces is undeniably extraordinary and has captured the attention of biologists, chemists, materials scientists, and engineers motivated by current limitations in adhesion technology. A byssus first appears as a single fiber called a drifting thread in the veliger stage of almost all bivalves where it functions like a kite tail to stabilize larval drift. Later, in settling pediveligers, byssal threads are produced as anchoring tethers to marine surfaces during metamorphosis into the adult form which, depending on the species, can possess or lack a byssus.[96] Indeed, in a smaller subset of mussel genera including *Mytilus* spp., the ability to produce a byssus is retained into adulthood where it enables colonization of intertidal zones with the highest wave impact.

Mytilus byssus adheres via a disc-like structure known as the plaque, into which the core fiber is rooted.[97,98] The wet adhesive strength of a single *M. californianus* plaque on glass pulled at 45° and at 30 µm/s ranges from 1 to 5 MN/m^2.[99] Similar adhesion is achieved on shell, wood pilings, various metal/minerals, plastic, and even non-polar surfaces such as Teflon.[100,101] This versatility in a hydrated, salt-encrusted, and corrosive environment has been a key factor in the evolutionary success of *Mytilid* mussels and a major driver of research into mussel-inspired glues with both technical and biomedical applications.[41] However, a fundamental understanding of the complex chemistry of the byssus plaque is incomplete and still holds many secrets.

Structural characterization

Early investigations of the internal structure of the plaque by Tamarin[97] and Waite[98] revealed a porous sponge-like architecture. At the interface with the substrate, the plaque was observed to form a thin dense layer, while the collagenous fibers of the core are anchored like tree roots in the spongy bulk of the

Fig. 6. Mytilus plaque structure and adhesion of Mfps. (A) Light stereomicroscopy image of plaque with attached thread from *M. californianus*; red bar indicates location of section. (B) Plaque section viewed by SEM showing two length scales of porosity at 2000 and 100 nm. Labels: outer cuticle (OC), spongy core (SC), collagen fibers (CF) and the continuous film at plaque interface (PI). (C) Higher magnification of the TEM plaque section (B, red box) featuring the 100 nm pores and continuous PI film. (D) Schematic of interfacial plaque protein distribution. The fine sub-100 nm mesh is thought to be hydrogel filled with coacervate droplets of mefp-3 and mfp-6, acting as a reducing reservoir against oxidative damage. (E) Measuring the adhesion of plaque proteins by SFA. Asymmetric and symmetric modes of mfp-3 application allow separate determination of adhesive and cohesive contributions from pull-off forces (F/R). (F) With asymmetric mode, force versus distance curves show significant pH dependence for adhesion and hardwall (i.e., how much a protein compresses). Adhesion decreases and hardwall increases as pH increases. (G) Nearly complete adhesion loss at pH 7.5 is attributed to Dopa oxidation, which cannot be restored by return to pH 5.5. However, addition of thiol-rich mfp-6 provides electrons for reduction of quinones to Dopa and restoration of adhesion. (H) Adhesion to mica (aluminosilicate) requires both the catechol moiety as in Dopa and a cationic sidechain like lysine (⊕) in 3-armed-TREN constructs. Having only one of these reduces adhesion to near control levels. Lysyl-ammonium evicts hydrated surface cations opening the door for catechol-binding to oxides and (or) metals. Labels: stalk (|) to ⊕ is long (Lys) or short (Orn); stalk only has no cation; stalk with circle is an acetylated amine. Panels (C) and (D) adapted from Valois et al. 2020[103] with permission, panels (F) and (G) adapted from Yu et al. 2011[104] with permission, and panel H adapted from Maier et al. 2015[105] with permission. [Colour online.]

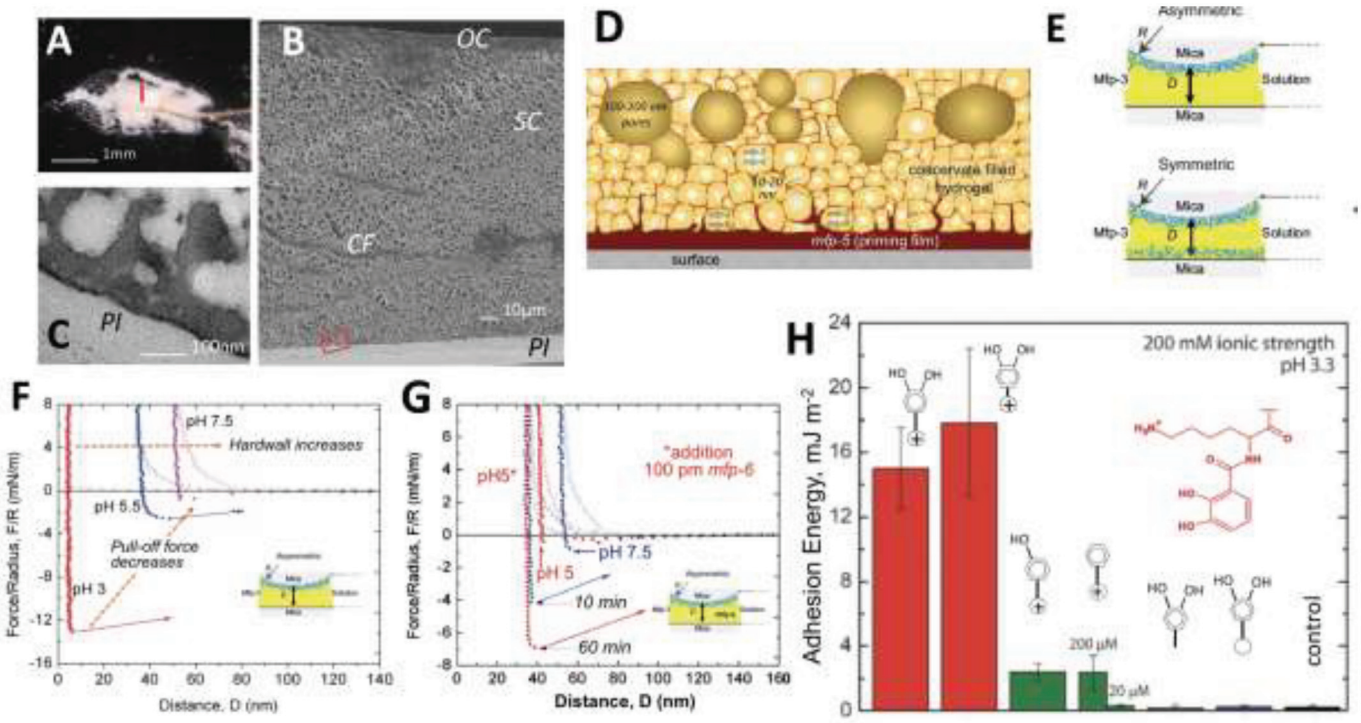

plaque. Subsequent work by Waite, Helgeson, and Valentine utilizing SEM and SANS revealed characteristic porosities of approximately 2 μm and 100 nm in the plaque interior (Figs. 6A–6C).[102] The specific localization of the different protein building blocks within the complex plaque structure has been an area of intense experimental effort with more details emerging over the last decade or so. Biochemical and spectroscopic investigations revealed that the bulk trabecular scaffold is comprised primarily of mfp-2, which consists of 11 tandem repeats of a ~45-residue long epidermal growth factor (EGF) motif and that these DOPA-rich proteins (~5 mol%) are cross-linked via DOPA–metal interactions (likely Fe/V and Ca).[106–108] Conversely, MALDI analysis of plaque footprints remaining after plaque removal showed that mfp-3, mfp-5, and mfp-6 were localized nearest the plaque–substrate interface.[35] Recent findings by Waite's group suggest that mfp-5 comprises the adhesive layer directly at the substrate interface, while the pores near the interface are filled with a fluid protein condensate containing mfp-3 and mfp-6 (Fig. 6D).[103] At the plaque–core interface, mfp-4 was proposed to comprise the biochemical linkage between the preCol fibers and mfp-2, although this was never specifically demonstrated.[109]

Compositional characterization

As mentioned above, Waite's group systematically identified and characterized six different proteins that were localized specifically to the plaque — mfp-2, mfp-3, mfp-4, mfp-5, mfp-6, and mfp-7,[28,31–33,36,109] whose defining properties are highlighted along with others in Table 1. More recently, transcriptomic analyses have suggested an additional 10 phenol gland proteins that might be present in the plaque (Table 1),[31] one of which has been confirmed via proteomics.[103] A common feature of most plaque proteins is the post-translational modification of tyrosine into DOPA ranging from 2 mol% for mfp-4 to 30 mol% for mfp-5,[110] but other modifications include phosphoserine and 4-hydroxyarginine. These proteins all tend to have basic isoelectric points, no doubt due to elevated arginine and lysine contents. Among the mfps confirmed in the plaque, mfp-6 is unusual in its high content of thiol/thiolate cysteines.[36,104] Of particular note, Waite's group and the group of Eli Sone also discovered homologous DOPA-rich proteins in the adhesive plaques of freshwater *Dreissenid* mussels (e.g., Zebra and Quagga mussels), suggesting that this biochemical adhesion strategy may be evolutionarily conserved across different orders of mussels.[111–113]

Table 1. Known (bolded) and putative (italicized) mussel foot proteins (MFPs) in *Mytilus* spp. byssus plaques and (or) the phenol gland.

MFP	Mass (kD)[a]	*pI*[b]	DOPA (mol%)	Variants	Miscellaneous	Ref.
1	110	10.5	10–15	2	$[decapeptide]_{75–80}$	25
2	45	9.5	5	4–5	$[EGF\ repeat]_{11}$	28
3 (S and F)	5–7	10.5	10–25	~30	HO-Arginine	32
4	93	8	2	1	15% His	109
5	9	9	30	1–2	10% pSer	33
6	11.5	9.5	5	5	11% Cys	36
7	4	10.9	? (Y 17)[c]	2	GKY; GGH repeats	31
8	4.8	10	? (Y 24)	1	$[GKY]_{10}$ repeat	31
9	11.4	9.8	? (Y 8)	2	H_6 and H_3	31
10	35	8.5	? (Y 11)	1	96 AA repeat	31
11	57	10	? (Y 11)	3	$[GH]_{30}$ repeat	31
12	80	9	? (Y 12)	1	$[RR, KK, KR]_{17}$	31
13	13	10.4	? (Y 16)	1	10% Cys	31
14	10.6	8.5	? (Y 3)	1	10% Cys	31
15	27	9.5	5 (Y 9)	1	6% Cys	31

[a]Average mass in K Daltons was estimated experimentally or predicted from deduced sequence.
[b]Iso-electric point was experimentally determined or predicted from amino acid pK_as.
[c]In the case of transcriptome-deduced sequences Dopa is unknown but Y provides an upper limit.

Structure–function relationships

Considering the large number of proteins in the byssus plaque, delineating clear structure–function relationships for specific proteins has been challenging. A shared trait of the most prominent interfacial proteins is high DOPA content — up to 30 mol%. That the DOPA catechol moiety might be the smoking gun of adhesion was first floated in 1981.[84] In 1987, as a predecessor to the synthetic mussel-inspired adhesives that would emerge decades later, Yamamoto demonstrated for the first time that synthetic DOPA-containing peptides modeled after mussel protein motifs could mediate adhesion on metal oxide surfaces.[114] In the early 2000s, the northwestern group led by Messersmith directly tested the hypothesis that single catechol groups could mediate surface adhesion on metal oxide surfaces using AFM based single molecule force spectroscopy, revealing that the interaction was strong (up to 900 pN), yet completely reversible over hundreds of cycles when shielded from oxidation.[40]

While this specific focus on the catechol moiety of DOPA provided crucial new insights, the deeper question of how the specific plaque proteins interact with the surfaces remains debated. Between 2007 and 2017, the Waite and Israelachvilli groups chipped away at this puzzle through an interdisciplinary approach combining classical biochemical analysis with advanced surface science.[106,115–123] Methodology critical to this approach was the surface forces apparatus (SFA) — an experimental platform developed by Israelachvilli capable of measuring adhesive and cohesive forces of molecules, including proteins, with 1 Å distance and 0.1 nano Newton force accuracy.[124,125] The different byssus plaque proteins were systematically investigated in both symmetric and asymmetric measurement modes to probe cohesion and adhesion (Fig. 6E), respectively, revealing that certain plaque proteins such as mfp-3 and mfp-5 are superior at bridging between two surfaces (usually mica),[115,123] while others such as mfp-2 (and the cuticle protein mfp-1) are inferior adhesives but reveal large cohesive improvements in the presence of metal ions.[94,106] These observations are consistent with the localization of mfp-3 and mfp-5 positioned at/near the substrate interface[35] and mfp-2 in the trabeculae of the porous plaque structure[106] — corroborating their proposed function in plaque adhesion and cohesion, respectively. While adhesion was initially thought to be mediated via chelation of metals in the metal oxide surfaces by the DOPA oxygen groups, the fact that strong adhesion is observed at acidic pH, suggests that H-bond and coulombic interactions are also key contributors in the surface chemistry.[122] Moreover, it was observed that the mussel proteins are highly versatile and may interact with non-polar surfaces via hydrophobic forces.[119,121]

The SFA also revealed the extreme pH-dependence of adhesion in experiments with individual proteins (Fig. 6C), as well as the role of protein mixtures to enable adhesion under natural conditions (e.g., pH 7–8). The conspicuous cysteine residues of mfp-6 were particularly crucial in maintaining adhesion in marine environments.[104] It is well documented that DOPA has a strong tendency to oxidize from its catechol to its quinone form under the basic conditions present in seawater. Moreover, Messersmith's single molecule force measurements revealed that the quinone form is much less effective at adhering to anything but amine-modified surfaces,[40] and SFA experiments by Waite and Israelachvilli showed a large decrease in adhesive energy for mfp-3 and mfp-5 under basic conditions.[122,126] Given the alkaline pH of seawater, one would predict that DOPA would be ineffective at sticking to surfaces under these conditions due to rampant DOPA oxidation. Indeed, Waite's group demonstrated that mfp-3 and -5 adhesion losses at pH 7.5 were correlated to Dopa oxidation (Fig. 6F); however, the losses were easily recovered, not by returning conditions to acidic pH, but rather by reductive restoration of Dopa-quinone to Dopa.[104,115] With its reservoir of cysteine thiols, mfp-6 proved to be an ideal interfacial antioxidant maintaining mfp-3 adhesion at pH 7.5 by reductive electron exchange (Fig. 6G).[104] Based on these observations, interfacial mfp-6 appears to be an adaptation for maintaining catechol-mediated adhesion in an oxidizing environment — a strategy that could be critical for future mussel-inspired adhesives as well.

While DOPA has received the most attention in synthetic biomimetic circles, subsequent scrutiny of plaque Mfp sequences showed other amino acids to be important. For example, DOPA residues in the adhesive proteins mfp-3 and mfp-5 (as well as in the cuticle protein mfp-1) are very often situated beside a positively charged amino acid — lysine or arginine.[33,84,110] Waite and Israelachvili teamed up with Butler to explore the functional implications of this phenomenon using model molecules and found that the presence of a cationic amine group in close proximity with catechol significantly enhances adhesion to aluminosilicates like mica (Fig. 6H).[105] This 1–2 synergy arises by dint of the charged amine's eviction of hydrated cations in the electric double layer on mica surfaces, clearing up binding sites by, for example, chelation on the surface for the catechol.

While molecular studies like these have yielded many compelling insights, collaborative work by Waite and Valentine on the native plaque adhesion provided a sobering epilogue to single Dopa, even single protein adhesion results.[99] When plaque adhesion to mica or glass was measured to break at 45°, the fracture energy (95 J m^{-2}) was shown to be nearly 5000-fold greater than the best performance of mfp-5 adhesion (~20 mJ m^{-2}). This is an eloquent reminder of the pitfalls of reductionism and a hint of how important molecular interactions between the interface and supramolecular architectures may be.

Fabrication of the byssus

As seen above, the structure–function relationships defining the remarkable properties of the byssus arise largely from the complex hierarchical organization of around 20 different protein precursors and a delicate balance of covalent and non-covalent cross-linking. While reductionist approaches to mimic the chemistry of the byssus have been successful by focusing expressly on DOPA and histidine moieties,[41,43] most of these mussel-inspired materials achieve neither the structural complexity nor the mechanical prowess of the native byssus. Thus, there has recently been a renewed interest in understanding the byssus fabrication process to elucidate how this complex structure is achieved in the first place. However, this is by no means a new area of research. The ability of mussels to rapidly fashion tough anchoring fibers has fascinated researchers for more than three centuries,[3,6] leading to focused investigation of the organ responsible for forming the byssus, which is known as the foot. The foot — tongue-like in appearance — ventures outside the shell during the thread-formation process, extending by several times its initial length as it searches for a suitable location to lay down a thread (Fig. 3),[127,128] Once the mussel commits, the foot firmly attaches to the surface, undergoing rhythmic muscular contractions for about 3–5 min, after which it releases a fully formed and functional thread. Hidden from the view of curious researchers, a complex process not dissimilar from polymer injection molding is taking place at the cellular to organ level.

Early anatomical and histological studies of the foot by Brown, Pujol, and Smyth provided evidence that the organ is a fully equipped byssus forming factory.[11,22,62] Running along the ventral surface of the foot is a narrow groove beginning at the base and terminating at the tip of the foot in a cup-like divot known as the distal depression.[129] Histological analysis of dissected foot tissue revealed the presence of several secretory glands surrounding the foot groove and distal depression, which comprises much of the foot tissue volume.[6,22] In the 1950s to 1960s, histochemical studies of the mussel foot[11,22] converged on the identification of three glands in the foot: the white, phenol, and enzyme glands. Later, based on more specific cytological criteria these were renamed — the collagen gland, the enzyme (or accessory) gland, and the phenol gland as described below (Figs. 3 and 7A). In the seventies and early eighties, the groups of Tamarin, Bairati, and Vitellaro-Zuccarello explored the ultrastructure of the various byssus glands using TEM.[63,71,92,97,129] Of the three glands that had been identified histologically, each was packed with cells containing massive quantities of micron-sized secretory vesicles, and the vesicles in each gland possessed a unique morphology and ultrastructural features (Fig. 7). The foot glands and their vesicles went relatively unstudied for nearly 40 years with few new insights, but recently, several studies from the groups of Waite and Harrington have again focused on understanding the byssus assembly process from a more dynamic perspective than these earlier studies and armed with a deeper understanding of the biochemistry than existed at that time.[80,90,103,108,110,127,130–133] Indeed, there is an obvious disparity between the nearly 20 proteins identified through biochemical and "-omic" analysis and the three secretory vesicle types currently characterized, implying either that there are multiple different proteins in each vesicle type, that there are more than three different types of vesicles, or most likely, that there is a combination of both scenarios.

F7

Collagen gland (core)

The largest of the three glands in the foot is responsible for forming the core running from the base of the foot to the distal depression surrounding the groove. This was the white gland initially identified by Tullberg in 1877;[6] however, the revelation that the vesicles within the gland contained collagenous proteins, led to the renaming as the collagen gland by Pujol in 1967[62] and later as the core gland based on the part of thread, which it forms.[127] The vesicles of the collagen gland possess elliptical shapes with a long axis of 1.5–2 μm (Fig. 4C).[63,130,132] The vesicles stain positively for collagen using Masson's trichrome and Sirius red staining and exhibit a strong birefringence indicating a high degree of molecular alignment.[127,132] Using TEM, both Tamarin and Vitellaro-Zucarello highlighted the characteristic banding pattern of dark and light staining layers with a periodicity of ~180 nm, with the dark-staining layers exhibiting a filamentous texture (Fig. 4C).[63,129,130] These studies were followed 40 years later by Harrington's group use of FIB-SEM, revealing the three-dimensional structure of the layers and confirming a long-standing hypothesis that the preCols are stored as a smectic mesophase within the vesicles, with clear disclinations.[130] It was hypothesized that this smectic LC, which has not been reported in other systems in nature, arises from the pentablock copolymer-like distribution of charge and hydropathy of the preCols, and that the smectic phase combines the fluidity required to mold the fiber during thread fabrication with the molecular alignment required to achieve the high degree of hierarchical structure observed in the native thread.[67,130] While this has proved challenging to confirm in vivo, there is substantial evidence in vitro and in situ that this is the case. Tamarin demonstrated that mussels could be induced to secrete byssus vesicles via injection of KCl into the pedal ganglion at the base of the foot.[129] Harrington's group showed thread induction resulted in the coalescence of the contents of the collagen vesicles into an immature fiber showing birefringence and, thus, alignment of preCols over hundreds of microns.[127] It was suggested that mechanical forces are required to achieve the high degree of molecular alignment observed in the native threads. Indeed, Harrington and Waite showed that purified preCols can be easily drawn into aligned fibers with native-like properties by simple mechanical drawing from dilute solutions,[78,79] while purified core vesicles could be formed into fibers through applied shear forces.[132]

Another question that has attracted much recent attention is how the preCol LC phase transitions rapidly from a liquid to a solid. Evidence supports the hypothesis initially proposed by Waite that this may in part be initiated by a pH transition going from the acidic storage conditions of the vesicle to the basic conditions of seawater and that the histidine residues in the termini of the preCols are key players in this process due to their pK_a of ~6.5.[30,78] In support, Harrington's group has showed recently that peptides based on histidine-rich domain (HRD) sequence undergo a transition into an amyloid-like structure when the pH is increased and can be used to initiate self-assembly of materials.[134–137] While initially it was proposed that metal ions might be critical as cross-linking agents in this process, these studies demonstrated that metal ions are not required at least in vitro. However, there is far more to be elucidated concerning this mechanism.

Enzyme or accessory gland (cuticle)

After the collagenous core is secreted and formed during the thread fabrication process, it is surmised that the thin protective cuticle is laid down from vesicles in a separate gland. Smyth's finding that polyphenoloxidase activity and catechols were colocalized in a

J_ID: CJC ART NO: cjc-2021-0191 Date: 10-January-22 Page: 12 Total Pages: 16 4/Color Figure(s): "F1-F7"

Fig. 7. Byssus fabrication overview. (A) Light microscopy image of a stained histological section of a mussel foot (left) with different glands identified schematically (right). Magnification of cuticle, core, and plaque vesicles are shown. (B) Three-dimensional reconstruction of serial sections similar to (A) along the whole length of the mussel foot showing gland distribution. (C)–(E) TEM images of vesicles used to form (C) core, (D) cuticle, and (E) plaque. (F) Schematic overview of thread secretion resembling injection molding, highlighting passive, and active aspects of the assembly process. Panels (A), (B) and (F) adapted from Priemel et al. 2017[127] under the creative commons license (CC BY 4.0), panel (D) adapted from Jehle et al. 2020[80] under the creative commons license (CC BY 4.0), and panels (C) and (E) kindly provided by Franziska Jehle. [Colour online.]

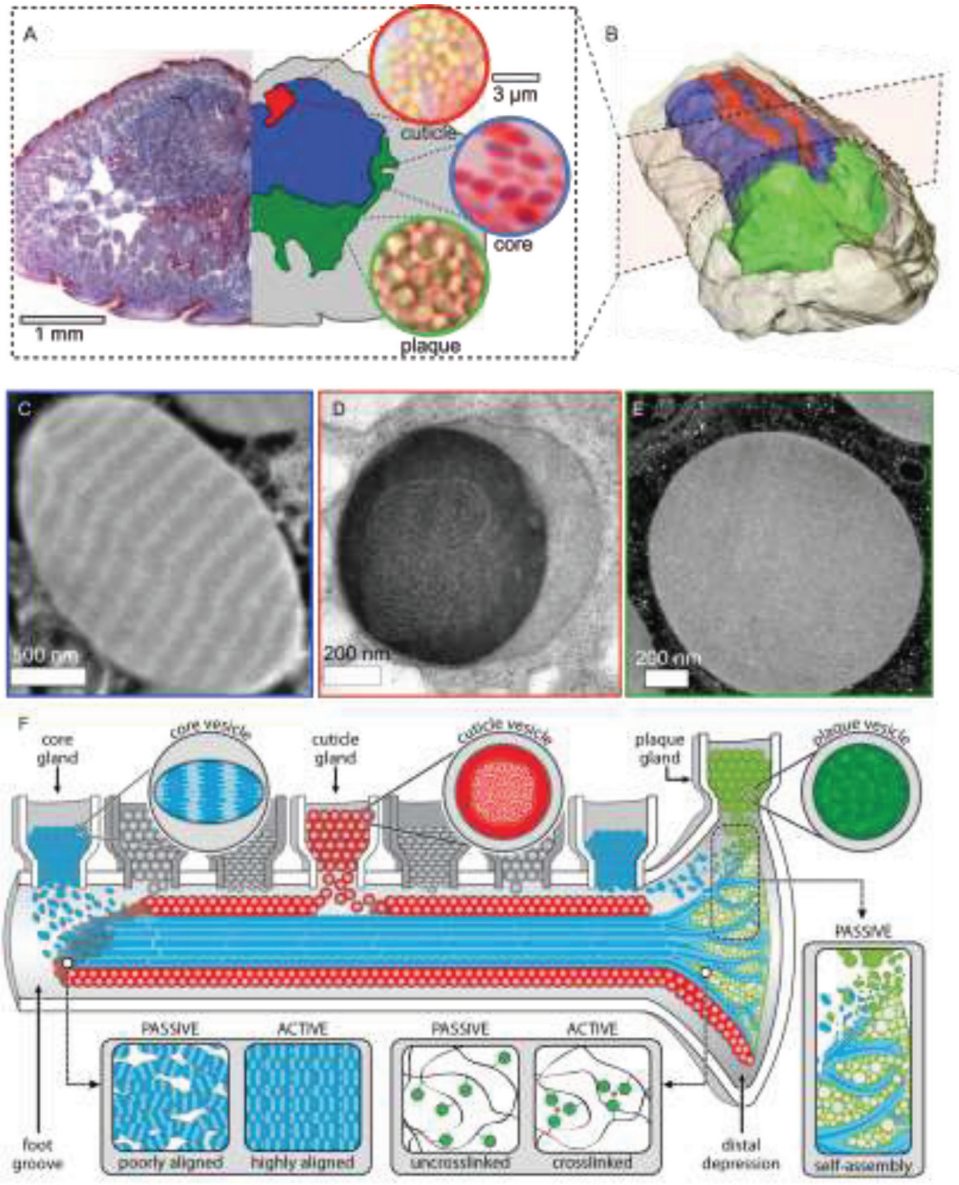

long slender bi-lobed gland along the ventral groove prompted him to refer to this as the enzyme gland (EG).[22] The polyphenoloxidase has been partially characterized,[23] but as typical for others of this type,[138] it is highly labile even after partial purification. Later work by Allen led to relabeling of the gland as "accessory gland".[48] Vitellaro-Zuccarello, however, concluded correctly that these vesicles contained structural proteins for building the cuticle due to the morphological similarity in TEM imaging of the vesicles and cuticle, stating "the EG does not completely deserve its name".[92] Harrington later rechristened it as the cuticle gland,[127] although all three monikers can still be found throughout the literature.

Early TEM analysis of the vesicles from *M. galloprovincialis* showed a biphasic internal texture resembling a brain-like whorled structure based on differential staining of two different components (Fig. 7D).[92] Interestingly, analysis of the cuticle forming vesicles from *M. californianus* by Tamarin also showed a biphasic structure but with lighter staining droplets present in a heavily stained continuous phase.[129] For nearly 40 years, this initial TEM work remained the only focused investigation of the vesicles responsible for forming the cuticles until the topic was revisited independently by the groups of Waite and Harrington. Monnier and Waite revealed that different mussel species have vesicles with different nanoscale textures with two differently staining phases observed but always showing evidence of phase separation.[93] Nanoscale compositional analysis of *M. edulis* vesicles by Harrington's group that the brain-like phase given the name protogranule is

enriched in DOPA-rich proteins (i.e., mfp-1) while the outer phase termed the protomatrix is enriched in sulfur,[80] presumably comprised of putative Cys-rich proteins observed in transcriptomic studies.[31] During induced secretion, it was observed that the protomatrix of the secreted vesicle contents fuse and spread over the surface of the already formed core with the protogranules remaining as separate entities producing a cohesive coating on the core. Notably, the vesicles do not show DOPA–metal coordination, indicating that metal ions are added separately.[80] The forces driving phase separation are still unclear, but one compelling hypothesis posits that the nonrepetitive and slightly less polar tail of mefp-1 (Fig. 5H) might drive phase separation when mixed with the Cys-rich matrix proteins in block-copolymer like behavior.[80] In addition, cation–π interactions are powerful initiators of mfp-1 phase separation in vitro.[139]

Phenol gland (plaque)

The phenol gland, originally part of the purple gland in Tullberg's analysis (the other part being the accessory gland), is comprised of cells filled with spherical vesicles (1.5–2 μm) that appear homogenous in TEM imaging and are secreted into the distal depression of the foot, forming the adhesive plaque (Fig. 7E).[61,97,129,139] For this reason, it has also more recently been referred to as the plaque gland.[127] Early histological analysis of the gland suggested the presence of proteins rich in phenolic amino acids from which the gland's name is derived,[11,22,140] which is consistent with the later biochemical studies of Waite described above. Currently, little is understood about the exact contents of the vesicles in the phenol gland, however, considering the sheer number of different plaque proteins and their precise localization within the plaque structure, it seems plausible that there are multiple variants of the plaque-forming vesicles stored in the phenol gland, each containing different assortments of plaque proteins. However, this conjecture remains be substantiated. Nonetheless, several studies have shown that the proteins in the plaque vesicles are stored under very acidic pH conditions (pH 2) and under reducing conditions.[127,131,133] As posited initially by Waite, these conditions likely provide a controlled microenvironment conducive to DOPA catechol storage and adhesion.[110]

The fabrication process by which the plaque proteins transform from vesicle to adhesive has received less attention than the proteins themselves. Tamarin showed in 1976 that there are cilia-lined channels running through the phenol gland termed the longitudinal ducts (LDs), and that during induced thread formation, the contents of the vesicles are secreted through the LDs into the distal depression.[97] For nearly 50 years, there was not much further analysis of the LDs until very recent work by Harrington's group, which combined histology, confocal Raman imaging, TEM, and FIB-SEM to follow the plaque formation.[108] Most interesting was the discovery of the metal storage particles (MSPs), which contain concentrated Fe and V stabilized by catechol coordination. Assembly studies revealed that the MSPs are mixed with the secreted plaque proteins within the lumen of the LDs in which the proteins gradually cross-link with the metal ions via DOPA residues hardening on their way to the distal depression.[108] This microfluidic-like process by which the metals are introduced into the plaque holds great potential for inspiring future advances in mussel-inspired materials.

Continuing the thread: closing remarks and ruminations

The story of human fascination with the mussel byssus is a long one dating back to Aristotle and the ancient Greeks, continuing with stops and starts passing through France, Germany, Italy, and the UK, while currently concentrated at the sunny coast of Santa Barbara and the icy Atlantic waters of Québec. Early scientific interest in mussel byssus was stoked by serendipitous errors, a rich legacy of natural history, the exigencies of the War and insights by Brown, Picken, and Pryor who merged curiosity, scholarship, and a readiness to cross disciplinary boundaries. The biomimetics of the 1940s are particularly interesting, not only because biology inspired new technologies such as aircraft construction, but also because when those technologies became passé, the biology did not. Indeed, the legacy of these trailblazers continues to rouse and inspire the current and future generation of biological materials scientists to uncover the secrets of materials such as mussel byssus, spider silk,[141] velvet worm slime,[142] or hagfish slime,[143] providing extractable chemical design principles for driving development and sustainable production of next-generation polymers, adhesives, composites, and coatings. Along these lines, the dynamic feedback loop between fundamental investigation of biological mechanisms of materials formation/function and the efforts to engineer synthetic bio-inspired materials provides the momentum that drives this field forward. Thus, the story told in this review is only half the story, and we direct readers to several excellent reviews on mussel-inspired materials that tell the rest.[41–43]

Finally, it behooves us to emphasize that *Mytilus* spp. byssus represents an infinitesimal fraction of the diversity of biological materials in nature. Over 70 years of focused research on this material has yielded a deep, yet still growing understanding of these fibers, their function and their formation. By comparison, much less is known about the byssal threads of other mussel orders such as Ostreida (including *Pinna nobilis*)[144] and freshwater invasive species from *Dreissena* spp.[111,112] Given the variation between fibers from different *Mytilus* species, many exciting insights are yet to be discovered by studying the byssus fibers from other mussel orders. Thus, we end with a call to expand the exploration beyond the *Mytilus* byssus. Who knows where the story will end if we continue to follow the beckoning threads.

References

(1) Maeder, F. In: Maeder, F.; Hänggi, A.; Wunderlin, D., editors. Muschelseide – goldene Fäden vom Meeresgrund. 5 Continents, Milan. 2004. pp. 9–28.
(2) Van der Feen, P. J. *Basteria* **1949**, *13*, 66.
(3) Réaumur, R.-A. *Mémoires de mathématique et de physique de l'Académie royale des sciences*. 1711.
(4) de Heide, A. *Anatomie Mytuli, belgice mossel*. Amstelodami. 1684.
(5) Mueller, A. *Weigmann's Archiv fuer Naturgeschichten* **1837**, *3*, 1.
(6) Tullberg, T. *Nova Acta Regiae Societatis Upsaliensis* **1877**, *18*.
(7) Seydel, E. *Zoologisch. Jahrb*. **1909**, *27*, 461.
(8) Stary, Z.; Andratschke, I. *Z. Physiol. Chem*. **1925**, *148*, 83.
(9) Astbury, W. T.; Bell, F. O. *Nature* **1940**, *145* (3672), 421. doi:10.1038/145421a0.
(10) Champetier, G.; Faure-Fremiet, E. *C.R. Acad. Sci. Paris* **1938**, *207*, 1133.
(11) Brown, C. H. *Q. J. Microsc. Sci*. **1952**, *93* (4), 487.
(12) Gordon, J. E. The new science of strong materials. Princeton Paperbacks, Princeton, NJ. 1968.
(13) Widdess, R. *Proc. Br. Acad*. **2010**, *166*, 227.
(14) Pryor, M. G. M.; Imms, A. D. *Proc. R. Soc. B* **1940**, *128* (852), 378.
(15) Hackman, R. H.; Todd, A. R. *Biochem. J*. **1953**, *55* (4), 631. doi:10.1042/bj0550631.
(16) Pryor, M. G.; Russell, P. B.; Todd, A. R. *Biochem. J*. **1946**, *40* (5–6), 627.
(17) Vincent, J. F. V. *J. Adhes*. **2009**, *85* (11), 755. doi:10.1080/00218460903291296.
(18) Brown, C. H. *Nature* **1950**, *165* (4190), 275. doi:10.1038/165275b0.
(19) Brown, C. H. *Q. J. Microsc. Sci*. **1950**, *91* (3), 331.
(20) Brown, C. H. *J. Cell Sci*. **1955**, *s3-96* (36), 483.
(21) Brown, C. H. Structural materials in animals. Pitman, London, UK. 1975.
(22) Smyth, J. D. *Q. J. Microsc. Sci*. **1954**, *95* (2), 139.
(23) Waite, J. H. *J. Mar. Biol. Assoc. UK* **1985**, *65* (2), 359.
(24) Arnow, L. E. *J. Biol. Chem*. **1937**, *118* (2), 531. doi:10.1016/S0021-9258(18)74509-2.
(25) Taylor, S. W.; Waite, J. H.; Ross, M. M.; Shabanowitz, J.; Hunt, D. F. *J. Am. Chem. Soc*. **1994**, *116* (23), 10803. doi:10.1021/ja00102a063.
(26) Waite, J. H. *J. Biol. Chem*. **1983**, *258* (5), 2911.
(27) Miki, D.; Takeuchi, Y.; Inoue, K.; Odo, S. *Biol Bull*. **1996**, *190* (2), 213. doi:10.2307/1542541.
(28) Rzepecki, L. M.; Hansen, K. M.; Waite, J. H. *Biol. Bull*. **1992**, *183* (1), 123. doi:10.2307/1542413.
(29) Inoue, K.; Takeuchi, Y.; Miki, D.; Odo, S. *J. Biol. Chem*. **1995**, *270* (12), 6698. doi:10.1074/jbc.270.12.6698.
(30) Waite, J. H.; Qin, X.-X.; Coyne, K. J. *Matrix Biol*. **1998**, *17* (2), 93. doi:10.1016/S0945-053X(98)90023-3.

(31) DeMartini, D. G.; Errico, J. M.; Sjoestroem, S.; Fenster, A.; Waite, J. H. *J. R. Soc. Interface* **2017**, *14* (131), 20170151. doi:10.1098/rsif.2017.0151.
(32) Papov, V. V.; Diamond, T. V.; Biemann, K.; Waite, J. H. *J. Biol. Chem.* **1995**, *270* (34), 20183. doi:10.1074/jbc.270.34.20183.
(33) Waite, J. H.; Qin, X. X. *Biochemistry* **2001**, *40* (9), 2887. doi:10.1021/bi002718x.
(34) Inoue, K.; Takeuchi, Y.; Miki, D.; Odo, S.; Harayama, S.; Waite, J. H. *Eur. J. Biochem.* **1996**, *239* (1), 172. doi:10.1111/j.1432-1033.1996.0172u.x.
(35) Zhao, H.; Robertson, N. B.; Jewhurst, S. A.; Waite, J. H. *J. Biol. Chem.* **2006**, *281* (16), 11090. doi:10.1074/jbc.M510792200.
(36) Zhao, H.; Waite, J. H. *J. Biol. Chem.* **2006**, *281* (36), 26150. doi:10.1074/jbc.M604357200.
(37) Harrington, M. J.; Masic, A.; Holten-Andersen, N.; Waite, J. H.; Fratzl, P. *Science* **2010**, *328*, 216. doi:10.1126/science.1181044.
(38) Holten-Andersen, N.; Harrington, M. J.; Birkedal, H.; Lee, B. P.; Messersmith, P. B.; Lee, K. Y. C.; Waite, J. H. *Proc. Nat. Acad. Sci. U.S.A.* **2011**, *108* (7), 2651. doi:10.1073/pnas.1015862108.
(39) Taylor, S. W.; Chase, D. B.; Emptage, M. H.; Nelson, M. J.; Waite, J. H. *Inorg. Chem.* **1996**, *35* (26), 7572. doi:10.1021/ic960514s.
(40) Lee, H.; Scherer, N. F.; Messersmith, P. B. *Proc. Nat. Acad. Sci. U.S.A.* **2006**, *103* (35), 12999. doi:10.1073/pnas.0605552103.
(41) Lee, B. P.; Messersmith, P. B.; Israelachvili, J. N.; Waite, J. H. *Annu. Rev. Mater. Res.* **2011**, *41*, 99. doi:10.1146/annurev-matsci-062910-100429.
(42) Krogsgaard, M.; Nue, V.; Birkedal, H. *Chem. Eur. J.* **2016**, *22* (3), 844. doi:10.1002/chem.201503380.
(43) Khare, E.; Holten-Andersen, N.; Buehler, M. J. *Nat. Rev. Mater.* **2021**, *6* (5), 421. doi:10.1038/s41578-020-00270-z.
(44) Reinecke, A.; Bertinetti, L.; Fratzl, P.; Harrington, M. J. *J. Struct. Biol.* **2017**, *196*, 329. doi:10.1016/j.jsb.2016.07.020.
(45) Bell, C. *J. Exp. Mar. Biol. Ecol.* **1994**, *181* (1), 9. doi:10.1016/0022-0981(94)90101-5.
(46) Carrington, E. *Integr. Compar. Biol.* **2002**, *42* (4), 846. doi:10.1093/icb/42.4.846.
(47) Mercer, E. H. *Aust. J. Mar. Freshw. Res.* **1952**, *3* (2), 199. doi:10.1071/MF9520199.
(48) Allen, J. A.; Cook, M.; Jackson, D. J.; Preston, S.; Worth, E. M. *J. Mollusc. Stud.* **1976**, *42* (2), 279. doi:10.1093/oxfordjournals.mollus.a065333.
(49) Smeathers, J. E.; Vincent, J. F. V. *J. Mollusc. Stud.* **1979**, *45* (2), 219. doi:10.1093/oxfordjournals.mollus.a065497.
(50) Price, H. A. *J. Zool.* **1981**, *194* (2), 245. doi:10.1111/j.1469-7998.1981.tb05771.x.
(51) Bell, E.; Gosline, J. *J. Exp. Biol.* **1996**, *199* (4), 1005. doi:10.1242/jeb.199.4.1005.
(52) Carrington, E.; Gosline, J. *Am. Malacol. Bull.* **2004**, *18* (1–2), 135.
(53) Gosline, J.; Lillie, M.; Carrington, E.; Guerette, P.; Ortlepp, C.; Savage, K. *Phil. Trans. R. Soc. B* **2002**, *357*, 121. doi:10.1098/rstb.2001.1022.
(54) Waite, J.; Vaccaro, E.; Sun, C.; Lucas, J. *Phil. Trans. R. Soc. B* **2002**, *357* (1418), 143. doi:10.1098/rstb.2001.1025.
(55) Toffoli, A.; Bitner-Gregersen, E. M. Types of ocean surface waves, wave classification. In Encyclopedia of Maritime and Offshore Engineering. John Wiley & Sons, Ltd. 2017. pp 1–8.
(56) Harrington, M. J.; Waite, J. H. *J. Exp. Biol.* **2007**, *210* (24), 4307. doi:10.1242/jeb.009753.
(57) Vaccaro, E.; Waite, J. H. *Biomacromolecules* **2001**, *2* (3), 906. doi:10.1021/bm0100514.
(58) Zechel, S.; Hager, M. D.; Priemel, T.; Harrington, M. J. *Biomimetics* **2019**, *4* (1), 20. doi:10.3390/biomimetics4010020.
(59) Harrington, M. J.; Gupta, H. S.; Fratzl, P.; Waite, J. H. *J. Struct. Biol.* **2009**, *167* (1), 47. doi:10.1016/j.jsb.2009.03.001.
(60) Sun, C. J.; Vaccaro, E.; Waite, J. H. *Biophys. J.* **2001**, *81* (6), 3590. doi:10.1016/S0006-3495(01)75989-9.
(61) Price, H. A. *J. Mollusc. Stud.* **1983**, *49* (1), 9. doi:10.1093/oxfordjournals.mollus.a065695.
(62) Pujol, J. P. *Nature* **1967**, *214* (5084), 204. doi:10.1038/214204a0.
(63) Vitellaro-Zuccarello, L. *J. Ultrastruct. Res.* **1980**, *73*, 135.
(64) Coyne, K. J.; Qin, X.-X.; Waite, J. H. *Science* **1997**, *277* (5333), 1830. doi:10.1126/science.277.5333.1830.
(65) Qin, X. X.; Coyne, K. J.; Waite, J. H. *J. Biol. Chem.* **1997**, *272* (51), 32623. doi:10.1074/jbc.272.51.32623.
(66) Qin, X. X.; Waite, J. H. *J. Exp. Biol.* **1995**, *198* (3), 633. doi:10.1242/jeb.198.3.633.
(67) Hassenkam, T.; Gutsmann, T.; Hansma, P.; Sagert, J.; Waite, J. H. *Biomacromolecules* **2004**, *5* (4), 1351. doi:10.1021/bm049899t.
(68) Sagert, J.; Waite, J. H. *J. Exp. Biol.* **2009**, *212* (14), 2224. doi:10.1242/jeb.029686.
(69) Sun, C.; Lucas, J. M.; Waite, J. H. *Biomacromolecules* **2002**, *3* (6), 1240. doi:10.1021/bm0255903.
(70) Rudall, K. M. *Symp. Soc. Exp. Biol.* **1955**, *9*, 49.
(71) Bairati, A.; Zuccarello, L. V. *Cell Tiss. Res.* **1976**, *166*, 219. doi:10.1007/BF00227043.
(72) Bairati, A. J.; Zuccarello, L. V. *J. Submicr. Cytol.* **1974**, *6*, 367.
(73) Krauss, S.; Metzger, T. H.; Fratzl, P.; Harrington, M. J. *Biomacromolecules* **2013**, *14* (5), 1520. doi:10.1021/bm4001712.
(74) Hagenau, A.; Papadopoulos, P.; Kremer, F.; Scheibel, T. *J. Struct. Biol.* **2011**, *175* (3), 339. doi:10.1016/j.jsb.2011.05.016.
(75) Arnold, A. A.; Byette, F.; Seguin-Heine, M. O.; LeBlanc, A.; Sleno, L.; Tremblay, R.; Pellerin, C.; Marcotte, I. *Biomacromolecules* **2013**, *14* (1), 132.]doi:10.1021/bm301493u.
(76) Coombs, T. L.; Keller, P. J. *Aquat. Toxicol.* **1981**, *1* (5–6), 291. doi:10.1016/0166-445X(81)90023-0.
(77) Schmitt, C. N. Z.; Politi, Y.; Reinecke, A.; Harrington, M. J. *Biomacromolecules* **2015**, *16* (9), 2852. doi:10.1021/acs.biomac.5b00803.
(78) Harrington, M. J.; Waite, J. H. *Biomacromolecules*, **2008**, *9* (5), 1480. doi:10.1021/bm8000827.
(79) Harrington, M. J.; Waite, J. H. *Adv. Mater.* **2009**, *21* (4), 440. doi:10.1002/adma.200801072.
(80) Jehle, F.; Macías-Sánchez, E.; Sviben, S.; Fratzl, P.; Bertinetti, L.; Harrington, M. J. *Nat. Commun.* **2020**, *11* (1), 862. doi:10.1038/s41467-020-14709-y.
(81) Holten-Andersen, N.; Fantner, G. E.; Hohlbauch, S.; Waite, J. H.; Zok, F. W. *Nat. Mater.* **2007**, *6* (9), 669. doi:10.1038/nmat1956.
(82) Holten-Andersen, N.; Mates, T. E.; Toprak, M. S.; Stucky, G. D.; Zok, F. W.; Waite, J. H. *Langmuir* **2009**, *25* (6), 3323. doi:10.1021/la8027012.
(83) Holten-Andersen, N.; Zhao, H.; Waite, J. H. *Biochemistry* **2009**, *48* (12), 2752. doi:10.1021/bi900018m.
(84) Waite, J. H.; Tanzer, M. L. *Science*, **1981**, *212* (4498), 1038. doi:10.1126/science.212.4498.1038.
(85) Benedict, C. V.; Waite, J. H. *J. Morphol.* **1986**, *189* (2), 171. doi:10.1002/jmor.1051890207.
(86) Waite, J. H.; Rice-Ficht, A. C. *Biochemistry* **1989**, *28* (14), 6104. doi:10.1021/bi00440a056.
(87) Zhao, H.; Sun, C.; Stewart, R. J.; Waite, J. H. *J. Biol. Chem.* **2005**, *280* (52), 42938. doi:10.1074/jbc.M508457200.
(88) Taylor, S. W.; Ross, M. M.; Waite, J. H. *Arch. Biochem. Biophys.* **1995**, *324* (2), 228. doi:10.1006/abbi.1995.0035.
(89) Waite, J. H.; Saleuddin, A. S. M.; Andersen, S. O. *J. Comp. Physiol. B* **1979**, *130* (4), 301. doi:10.1007/BF00689847.
(90) Valois, E.; Hoffman, C.; Demartini, D. G.; Waite, J. H. *Langmuir* **2019**, *35* (48), 15985. doi:10.1021/acs.langmuir.9b01844.
(91) Schmitt, C. N. Z.; Winter, A.; Bertinetti, L.; Masic, A.; Strauch, P.; Harrington, M. J. *J. R. Soc. Interface* **2015**, *12* (110), 20150466. doi:10.1098/rsif.2015.0466.
(92) Vitellaro-Zuccarello, L. *Tissue Cell* **1981**, *13* (4), 701. doi:10.1016/S0040-8166(81)80007-9.
(93) Monnier, C. A.; DeMartini, D. G.; Waite, J. H. *Nat. Commun.* **2018**, *9* (1), 3424. doi:10.1038/s41467-018-05952-5.
(94) Zeng, H.; Hwang, D. S.; Israelachvili, J. N.; Waite, J. H. *Proc. Nat. Acad. Sci. U.S.A.* **2010**, *107* (29), 12850. doi:10.1073/pnas.1007416107.
(95) Mesko, M.; Xiang, L.; Bohle, S.; Hwang, D. S.; Zeng, H.; Harrington, M. J. *Chem. Mater.* **2021**, *33* (16), 6530. doi:10.1021/acs.chemmater.1c02063.
(96) Yonge, C. M. *J. Mar. Biol.* **1962**, *42*, 113. doi:10.1017/S0025315400004495.
(97) Tamarin, A.; Lewis, P.; Askey, J. *J. Morphol.* **1976**, *149* (2), 199. doi:10.1002/jmor.1051490205.
(98) Benedict, C. V.; Waite, J. H. *J. Morphol.* **1986**, *189* (3), 261. doi:10.1002/jmor.1051890305.
(99) Desmond, K. W.; Zacchia, N. A.; Waite, J. H.; Valentine, M. T. *Soft Matter* **2015**, *11* (34), 6832. doi:10.1039/C5SM01072A.
(100) Waite, J. H. *Integr. Comp. Biol.* **2002**, *42* (6), 1172. doi:10.1093/icb/42.6.1172.
(101) Aldred, N.; Ista, L. K.; Callow, M. E.; Callow, J. A.; Lopez, G. P.; Clare, A. S. *J. R. Soc. Interface* **2006**, *3* (6), 37. doi:10.1098/rsif.2005.0074.
(102) Filippidi, E.; DeMartini, D. G.; de Molina, P. M.; Danner, E. W.; Kim, J.; Helgeson, M. E.; Waite, J. H.; Valentine, M. T. *J. R. Soc. Interface* **2015**, *12* (113), 20150827. doi:10.1098/rsif.2015.0827.
(103) Valois, E.; Mirshafian, R.; Waite, J. H. *Sci. Adv.* **2020**, *6* (23), eaaz6486. doi:10.1126/sciadv.aaz6486.
(104) Yu, J.; Wei, W.; Danner, E.; Ashley, R. K.; Israelachvili, J. N.; Waite, J. H. *Nat. Chem. Biol.* **2011**, *7* (9), 588. doi:10.1038/nchembio.630.
(105) Maier, G. P.; Rapp, M. V.; Waite, J. H.; Israelachvili, J. N.; Butler, A. *Science* **2015**, *349* (6248), 628. doi:10.1126/science.aab0556.
(106) Hwang, D. S.; Zeng, H. B.; Masic, A.; Harrington, M. J.; Israelachvili, J. N.; Waite, J. H. *J. Biol. Chem.* **2010**, *285* (33), 25850. doi:10.1074/jbc.M110.133157.
(107) Sever, M. J.; Weisser, J. T.; Monahan, J.; Srinivasan, S.; Wilker, J. J. *Angew. Chem. Intl. Ed. Engl.* **2004**, *43* (4), 448. doi:10.1002/anie.200352759.
(108) Priemel, T.; Palia, G.; Förste, F.; Jehle, F.; Sviben, S.; Mantouvalou, I.; et al. *Science 2021*, *374* (6564), 206. doi:10.1126/science.abi9702.
(109) Zhao, H.; Waite, J. H. *Biochemistry* **2006**, *45* (47), 14223. doi:10.1021/bi061677n.
(110) Waite, J. H. *J. Exp. Biol.* **2017**, *220* (4), 517. doi:10.1242/jeb.134056.
(111) Gantayet, A.; Rees, D. J.; Sone, E. D. *Mar. Biotechnol.* **2014**, *16* (2), 144. doi:10.1007/s10126-013-9537-9.
(112) Gantayet, A.; Ohana, L.; Sone, E. D. *Biofouling* **2013**, *29* (1), 77. doi:10.1080/08927014.2012.746672.
(113) Rzepecki, L. M.; Waite, J. H. *Mol Mar. Biol. Biotechnol.* **1993**, *2* (5), 267.
(114) Yamamoto, H. *J. Chem. Soc., Perkin Trans. 1* **1987**, 613. doi:10.1039/p19870000613.
(115) Danner, E. W.; Kan, Y.; Hammer, M. U.; Israelachvili, J. N.; Waite, J. H. *Biochemistry* **2012**, *51* (33), 6511. doi:10.1021/bi3002538.

(116) Lu, Q.; Danner, E.; Waite, J. H.; Israelachvili, J. N.; Zeng, H.; Hwang, D. S. *J. R. Soc. Interface* **2013**, *10* (79), 20120759. doi:10.1098/rsif.2012.0759.
(117) Mirshafian, R.; Wei, W.; Israelachvili, J. N.; Waite, J. H. *Biochemistry* **2016**, *55* (5), 743. doi:10.1021/acs.biochem.5b01177.
(118) Nicklisch, S. C. T.; Das, S.; Martinez Rodriguez, N. R.; Waite, J. H.; Israelachvili, J. N. *Biotechnol. Prog.* **2013**, *29* (6), 1587. doi:10.1002/btpr.1810.
(119) Wei, W.; Yu, J.; Broomell, C.; Israelachvili, J. N.; Waite, J. H. *J. Am. Chem. Soc.* **2013**, *135* (1), 377. doi:10.1021/ja309590f.
(120) Wei, W.; Yu, J.; Gebbie, M. A.; Tan, Y.; Martinez Rodriguez, N. R.; Israelachvili, J. N.; Waite, J. H. *Langmuir* **2015**, *31* (3), 1105. doi:10.1021/la504316q.
(121) Yu, J.; Kan, Y.; Rapp, M.; Danner, E.; Wei, W.; Das, S.; et al. *Proc. Nat. Acad. Sci. U.S.A.* **2013**, *110* (39), 15680. doi:10.1073/pnas.1315015110.
(122) Yu, J.; Wei, W.; Menyo, M. S.; Masic, A.; Waite, J. H.; Israelachvili, J. N. *Biomacromolecules* **2013**, *14* (4), 1072. doi:10.1021/bm301908y.
(123) Lin, Q.; Gourdon, D.; Sun, C. J.; Holten-Andersen, N.; Anderson, T. H.; Waite, J. H.; Israelchvili, J. N. *Proc. Nat. Acad. Sci. U.S.A.* **2007**, *104* (10), 3782. doi:10.1073/pnas.0607852104.
(124) Israelachvili, J. N. *J. Coll. Interface Sci.* **1973**, *44* (2), 259. doi:10.1016/0021-9797(73)90218-X.
(125) Israelachvili, J. N. Intermolecular and surface forces. Academic Press. 2011.
(126) Yu, J.; Wei, W.; Danner, E.; Israelachvili, J. N.; Waite, J. H. *Adv. Mater.* **2011**, *23* (20), 2362. doi:10.1002/adma.201003580. PMID:21520458.
(127) Priemel, T.; Degtyar, E.; Dean, M. N.; Harrington, M. J. *Nat. Commun.* **2017**, *8*, 14539. doi:10.1038/ncomms14539. PMID:28262668.
(128) Waite, J. H. The formation of mussel byssus: anatomy of a natural manufacturing process. In: Structure, Cellular Synthesis and Assembly of Biopolymers. Case, S. T., editor. Springer Berlin Heidelberg, Berlin, Heidelberg. 1992. pp. 27–54.
(129) Tamarin, A.; Keller, P. J. *J. Ultrastruct. Res.* **1972**, *40* (3–4), 401. doi:10.1016/s0022-5320(72)90110-4. PMID:5051880.
(130) Jehle, F.; Priemel, T.; Strauss, M.; Fratzl, P.; Bertinetti, L.; Harrington, M. J. *ACS Nano* **2021**, *15* (4), 6829. doi:10.1021/acsnano.0c10457.
(131) Priemel, T.; Palia, R.; Babych, M.; Thibodeaux, C. J.; Bourgault, S.; Harrington, M. J. *Proc. Nat. Acad. Sci. U.S.A.* **2020**, *117* (14), 7613. doi:10.1073/pnas.1919712117.
(132) Renner-Rao, M.; Clark, M.; Harrington, M. J. *Langmuir* **2019**, *35* (48), 15992. doi:10.1021/acs.langmuir.9b01932.
(133) Rodriguez, N. R. M.; Das, S.; Kaufman, Y.; Israelachvili, J. N.; Waite, J. H. *Biofouling* **2015**, *31* (2), 221. doi:10.1080/08927014.2015.1026337.
(134) Jehle, F.; Fratzl, P.; Harrington, M. J. *ACS Nano* **2018**, *12* (3), 2160. doi:10.1021/acsnano.7b07905.
(135) Reinecke, A.; Brezesinski, G.; Harrington, M. J. *Adv. Mater. Interfaces* **2016**, *4*, 1600416. doi:10.1002/admi.201600416.
(136) Schmidt, S.; Reinecke, A.; Wojcik, F.; Pussak, D.; Hartmann, L.; Harrington, M. J. *Biomacromolecules* **2014**, *15* (5), 1644. doi:10.1021/bm500017u.
(137) Trapaidze, A.; D'Antuono, M.; Fratzl, P.; Harrington, M. J. *Eur. Polym. J.* **2018**, *109*, 229. doi:10.1016/j.eurpolymj.2018.09.053.
(138) Pau, R. N. *Biochim. Biophys. Acta* **1984**, *782* (4), 422. doi:10.1016/0167-4781(84)90049-6.
(139) Kim, S.; Yoo, H. Y.; Huang, J.; Lee, Y.; Park, S.; Park, Y.; et al. *ACS Nano*, **2017**, *11* (7), 6764. doi:10.1021/acsnano.7b01370.
(140) Pujol, J. P. *Bull. Soc. Linn. Normandie* **1967**, *8*, 308.
(141) Heim, M.; Keerl, D.; Scheibel, T. *Angew. Chem. Intl. Ed.* **2009**, *48* (20), 3584. doi:10.1002/anie.200803341.
(142) Baer, A.; Schmidt, S.; Haensch, S.; Eder, M.; Mayer, G.; Harrington, M. J. *Nat. Commun.* **2017**, *8* (1), 974. doi:10.1038/s41467-017-01142-x.
(143) Fudge, D. S.; Hillis, S.; Levy, N.; Gosline, J. M. *Bioinspir. Biomim.* **2010**, *5* (3), 035002. doi:10.1088/1748-3182/5/3/035002.
(144) Pasche, D.; Horbelt, N.; Marin, F.; Motreuil, S.; Macias-Sanchez, E.; Falini, G.; et al. *Soft Matter* **2018**, *14* (27), 5654. doi:10.1039/C8SM00821C.

AUTHOR QUERIES

Please answer all queries requiring corrections. Those left unanswered will be assumed to be correct.

AQ1: It seems that “Dopa” and “DOPA” have been used interchangeably? If so, please standardize all instances to one or the other.